

# A Robust Framework for Secure Cardiovascular Risk Prediction: An Architectural Case Study of Differentially Private Federated Learning

Rodrigo Tertulino<sup>a,\*</sup>, Laércio Alencar<sup>a</sup>

<sup>a</sup>Federal Institute of Education, Science, and Technology of Rio Grande do Norte (IFRN), Natal, 3030-290, RN, Brazil

## Abstract

Accurate cardiovascular risk prediction is crucial for preventive healthcare; however, the development of robust Artificial Intelligence (AI) models is hindered by the fragmentation of clinical data across institutions due to stringent privacy regulations. This paper presents a comprehensive architectural case study validating the engineering robustness of *FedCVR*, a privacy-preserving Federated Learning framework applied to heterogeneous clinical networks. Rather than proposing a new theoretical optimizer, this work focuses on a systems engineering analysis to quantify the operational trade-offs of server-side adaptive optimization under utility-prioritized Differential Privacy (DP). By conducting a rigorous stress test in a high-fidelity synthetic environment calibrated against real-world datasets (Framingham, Cleveland), we systematically evaluate the system's resilience to statistical noise. The validation results demonstrate that integrating server-side momentum as a temporal denoiser allows the architecture to achieve a stable F1-score of 0.84 and an Area Under the Curve (AUC) of 0.96, statistically outperforming standard stateless baselines. Our findings confirm that server-side adaptivity is a structural prerequisite for recovering clinical utility under realistic privacy budgets, providing a validated engineering blueprint for secure multi-institutional collaboration.

**Keywords:** Federated learning, Differential privacy, Cardiovascular disease, Adaptive optimization, System architecture, Synthetic data

## 1. Introduction

Cardiovascular diseases (CVDs) represent the leading global cause of death, responsible for an estimated 20.5 million deaths in 2021, a figure projected to surge past 23.6 million by 2030 [1, 2]. The overwhelming majority of these fatalities are attributable to acute events such as heart attacks and strokes, often the culmination of a confluence of behavioral and physiological risk factors, including hypertension, elevated cholesterol, diabetes, and diet. Notably, this escalating health crisis is not uniformly distributed; low and middle-income countries are disproportionately affected, accounting for over three-quarters of all CVD-related deaths [3]. Such scale and socioeconomic disparities underscore the urgent need for innovative strategies to assess risk and prevent early onset, as the ongoing rise in prevalence poses a critical challenge for public health systems worldwide.

Addressing this multifaceted issue requires concerted global action to promote heart-healthy lifestyles and ensure equitable access to early detection; otherwise, the human and economic toll will continue to mount, jeopardizing millions and straining healthcare resources [4]. In this landscape, the proliferation of Electronic Health Records (EHRs) has created vast datasets with the potential to revolutionize medical diagnostics through

machine learning (ML) [5]. Consequently, CVDs represent a critical domain where predictive modeling can significantly improve early detection and patient outcomes [6].

However, the sensitive nature of patient data, protected by regulations such as GDPR [7] in Europe and HIPAA [8] in the EUA, poses a significant barrier to traditional centralized ML approaches that require aggregating data in a single location. This privacy constraint often leaves valuable data siloed within individual hospitals and clinics, limiting the development of highly accurate and generalizable models [9].

To address data privacy challenges, Federated Learning (FL) has been introduced as a distributed ML approach [10]. Instead of moving sensitive data to a central server in the FL framework, a global model is sent to distributed clients (e.g., hospitals). Each client trains the model on its local data, and only the resulting model updates, such as weights or gradients, are sent back to the central server for aggregation. As a result, this process is repeated over several rounds, allowing for the creation of a robust global model collaboratively without exposing any raw patient information. Thus, the approach preserves data privacy and enables institutions to build more powerful models by leveraging a larger and more diverse collective dataset than any single institution could access alone [11].

The primary objective of this study is to implement and evaluate an FL model specifically designed for cardiovascular risk prediction. To this end, a network of five distinct clients, representing hospitals with independent local datasets, is developed to collaboratively train a shared prediction model. The over-

\*Corresponding author

Email addresses: rodrigo.tertulino@ifrn.edu.br (Rodrigo Tertulino), lapea@ifrn.edu.br (Laércio Alencar)

URL: ORCID: 0000-0002-7594-9312 (Rodrigo Tertulino)

arching goal is to demonstrate FL’s viability as a solution for healthcare institutions to share insights and improve diagnostic accuracy while ensuring data remains secure and on-premises.

Furthermore, the analysis is deepened by integrating Differential Privacy (DP) to mitigate potential information leakage from model updates. As a formal mathematical framework, DP provides strong, provable guarantees against the identification of individual data within a dataset [12]. Consequently, the proposed model applies local DP by injecting carefully calibrated statistical noise into client updates before they are transmitted to the server. A critical component of this investigation involves analyzing the trade-off between enhanced privacy and its impact on performance metrics such as accuracy, precision, and recall. Such analysis is crucial for determining whether a DP-enhanced FL model remains a viable and effective tool for deployment in real-world clinical settings.

This paper addresses this gap by presenting a comprehensive **architectural case study** of *FedCVR*, a deployment framework specifically designed to mitigate the "cost of privacy" in cardiovascular risk prediction. Unlike theoretical studies that propose novel optimizers in isolation, this work adopts a systems engineering perspective. **While generic adaptive optimizers (e.g., FedAdam, FedYogi) exist in the literature, their operational stability under the specific dual constraints of strict Differential Privacy and high-dimensional clinical heterogeneity remains an under-explored engineering challenge.** We rigorously validate how server-side adaptive mechanisms, specifically momentum, function as architectural components to filter DP noise. By treating the FL system as a complete engineering artifact, we provide a validated blueprint for the secure clinical deployment of FL systems.

The primary contributions of this paper are summarized as follows:

- **Robust Framework for Clinical Non-IID Data:** We develop FedCVR, a framework incorporating server-side adaptive optimization designed to mitigate gradient divergence caused by the statistical heterogeneity (Non-IID) inherent in multi-institutional medical data.
- **Comprehensive Benchmarking & Resilience:** We evaluate FedCVR against five distinct baselines: FedAvg, FedProx, FedCluster, FedAdagrad, and FedYogi. We demonstrate that the specific momentum-based tuning in FedCVR acts as a superior temporal denoiser, significantly outperforming both stateless and other adaptive optimizers in the presence of Differential Privacy (DP) noise.
- **Privacy-Utility Trade-off Analysis:** We provide a rigorous empirical analysis of the impact of DP noise on model utility. Unlike previous works that treat DP as a black box, we quantify the specific privacy budget ( $\epsilon$ ) required to maintain clinical viability (Recall/Sensitivity) without compromising patient anonymity.
- **Statistical Validation:** We report comprehensive performance metrics (F1-Score, AUC, Recall) validated through

independent runs ( $N = 5$ ) and statistical significance testing ( $p < 0.05$ ), ensuring reproducibility and confirming that the performance gains are not artifacts of random initialization.

This paper is structured as follows: Section 2 reviews the relevant literature on FL, contextualizing the work within the current state of the art. Section 3 provides a background study on FL, establishing its importance in privacy-sensitive domains. Section 4 distinguishes the framework from standard approaches, followed by Section 5, which details the specific architecture of the FedCVR aggregation model. Section 6 discusses data availability challenges in healthcare and justifies the approach of using generated data. Section 7 details the proposed methodology, including the dataset characteristics and the FL-DP implementation. Section 8 presents the empirical results from the experiments, featuring a comparative analysis of the baseline and DP-enhanced models. Section 9 discusses the broader implications of these findings, and finally, Section 10 concludes the paper and outlines potential directions for future research.

## 2. Related Work

Applying ML to large-scale EHRs holds immense potential for advancing Cardiovascular Disease (CVD) research [13]. However, progress is fundamentally constrained by the challenge of "data silos," where valuable clinical data remains fragmented across different institutions due to stringent privacy regulations and security concerns [14]. Additionally, data fragmentation limits the development of robust, generalizable models that perform well across diverse patient populations [15, 16].

Hence, it effectively addresses challenges such as inconsistent data quality, unbalanced datasets, and paramount privacy concerns by enabling collaborative ML across multiple sites without requiring the sharing of raw data. Thus, privacy-preserving characteristics are crucial for maintaining compliance with stringent regulations, including GDPR and HIPAA [17, 18]. A significant challenge in real-world FL is statistical heterogeneity, where data distributions differ substantially between institutions (i.e., data is non-IID). The work by [19] provides a demonstration of this issue and FL’s advantage. Their study on detecting hypertrophic cardiomyopathy found that models trained at a single institution generalized poorly when tested on data from another country. However, a multinational FL approach significantly improved the model’s generalizability, underscoring FL’s ability to create more robust models by leveraging diverse, international data sources.

A significant hurdle in medical research has traditionally been the acquisition of sufficiently large and diverse datasets for model training within individual institutions, often compounded by the complexities of privacy and data ownership associated with centralized patient data sharing [20]. FL offers a compelling solution by facilitating multi-institutional collaboration through distributed model training, where data remains localized with its owners, and only aggregated model updates are shared.

Studies have corroborated FL’s efficacy, demonstrating that it can achieve up to 99% model quality comparable to centralized approaches, even when training involves ten distinct institutions [21]. In this work [22], a global FL initiative leveraged data from 6,134 glioblastoma patients across 71 geographically diverse sites, resulting in a robust and generalizable model for glioblastoma sub-compartment detection. This emphasizes the critical role of diverse datasets in developing clinically impactful models. Similarly, FL’s diagnostic utility was validated in hypertrophic cardiomyopathy using M&M and ACDC datasets subsets, confirming performance comparable to centralized systems while upholding patient privacy [23]. Beyond data heterogeneity, the operational deployment of FL introduces more complex challenges related to resource constraints and data lifecycle management [24].

A significant hurdle is the computational heterogeneity among clients, where some institutions may lack the powerful GPUs required for local training of large models. To address this, [25] proposes CAFE AU LAIT. In this compute-aware framework, resource-constrained clients contribute by generating data, which is then used by a strong central server to participate in the federated training alongside more powerful clients. While this approach democratizes participation, it also highlights a potential performance gap between models trained on synthetic data versus those trained on real, local updates, presenting a clear trade-off between inclusivity and model utility.

Synthetic data has also been explored to solve another critical issue: data incompleteness. The FLIGAN framework, proposed by [26], leverages federated GANs to generate high-quality synthetic data that augments client datasets suffering from severe class imbalances or insufficient data volume. Their results show that this technique can significantly improve model accuracy, though it introduces additional computational overhead during training. Furthermore, the data lifecycle within a trained model is a growing concern, driven by regulations such as the "right to be forgotten." Naively retraining a model from scratch to unlearn a user’s data is computationally prohibitive. In response, efficient Federated Unlearning (FU) methods, such as QUICKDROP, have been developed that use a small, distilled synthetic dataset to approximate gradients, enabling rapid, computationally inexpensive removal of data from a global model [27].

A consistent theme throughout the literature is the advantage of FL in facilitating multi-institutional collaboration that would otherwise be impossible. Studies have shown that FL can achieve model quality comparable to centralized approaches, even across many participating sites, underscoring the critical role of diverse datasets in creating clinically impactful models. Beyond diagnostics, FL has been instrumental in advancing research on complex diseases, such as brain tumors, by enabling collaboration without disclosing private patient information [28].

Meanwhile, FL inherently provides a strong baseline for privacy by keeping data localized; the model updates are not immune to inference attacks [29]. Most of the cited works primarily focus on addressing the challenge of model performance under data heterogeneity. A critical, often unaddressed aspect,

noted as a limitation or future work in these studies, is the need for stronger mathematical privacy guarantees.

However, the challenge of data remaining in silos due to privacy concerns restricts its full potential in clinical applications. Researchers continue to highlight FL as a viable solution for the future of digital health, addressing these critical challenges [30]. While many studies propose FL as a solution for privacy in healthcare, there remains a significant gap in research that moves beyond standard FL to implement and empirically analyze the true performance-cost and practical viability of a system enhanced with formal privacy guarantees, such as DP. Additionally, the study aims to address this specific gap. We implement a federated framework for cardiovascular risk prediction and take the critical next step of integrating DP. The objective is to provide formal privacy assurances against inference attacks and to conduct a comparative analysis of the performance trade-offs. Thus, this work contributes to developing trustworthy and scalable Artificial Intelligence (AI) solutions for the healthcare sector by evaluating the real-world viability of a truly secure and privacy-preserving FL system.

### 3. Background Study of Federated Learning

FL is a decentralized ML paradigm that enables multiple participants to collaboratively train models without sharing their raw data. This approach is particularly advantageous in contexts involving sensitive information, such as electronic health records (EHRs) in healthcare, where data privacy is of utmost importance [31].

In FL, a central server coordinates the learning process by distributing a global model to clients (e.g., hospitals) that hold local data. Meanwhile, clients perform training locally and then send only model updates back to the server, preserving data privacy [32]. In an FL system, let  $N$  be the total number of participating clients, where each client  $i$  possesses a local dataset  $D_i$ . The primary objective is to train a global model with parameters  $w$  using data from all clients without ever moving the data from their local devices. The overall optimization goal is to minimize a global loss function  $F(w)$ , which is defined as the weighted average of the local loss functions  $F_i(w)$  for each client:

$$F(w) = \sum_{i=1}^N \frac{|D_i|}{|D|} F_i(w), \quad \text{where } |D| = \sum_{i=1}^N |D_i| \quad (1)$$

#### 3.1. Federated Learning Process

The FL training process is conducted through a series of iterative communication rounds between a central server and a subset of participating clients [33]. A typical round consists of the following steps:

1. **Initialization:** The process begins with the server initializing the global model with parameters  $w_0$ .
2. **Local Training:** In each communication round  $t$ , the server sends the current global model  $w^t$  to a selection of clients. Each client  $i$  then updates the model locally by

minimizing its local loss function  $F_i(w)$  on its own dataset  $D_i$ . Therefore, it is typically done by performing one or more steps of gradient descent, following the local update rule:

$$w_i^{(t+1)} = w_i - \eta \nabla F_i(w_i) \quad (2)$$

where  $\eta$  is the learning rate.

3. **Model Aggregation:** After local training, the participating clients send their newly updated model parameters,  $w_i^{t+1}$ , to the central server. The server then aggregates these updates to compute the new global model parameters for the next round,  $w^{(t+1)}$ :

$$w_{t+1} = \sum_{i=1}^N \frac{|D_i|}{|D|} w_i^{(t+1)} \quad (3)$$

4. **Global Model Update:** The resulting aggregated model  $w_{t+1}$  becomes the new global model and is distributed to clients for the subsequent communication round.

As a result, the iterative process of distribution, local training, and aggregation continues until the global model converges or meets the desired performance criteria.

## 4. Distinguishing FedCVR from State-of-the-Art Baselines

To articulate the engineering advantages of the proposed framework, it is necessary to distinguish FedCVR not only from the canonical Federated Averaging (FedAvg) but also from regularization-based, clustering-based, and other adaptive baselines used in this study. The distinctions are rooted in how each method handles the server-side aggregation state and responds to the noise introduced by Differential Privacy (DP).

### 4.1. Versus Stateless Aggregators (FedAvg and FedProx)

FedAvg and FedProx operate under a *stateless* server-level paradigm.

- **FedAvg** computes the global model simply as a weighted average of client updates. It treats every communication round as an independent event, lacking any "memory" of the optimization trajectory [10, 34]. In the presence of DP noise, this statelessness is detrimental: the random Gaussian noise added in round  $t$  directly impacts the model  $w_{t+1}$  without any historical smoothing, leading to erratic convergence.
- **FedProx** improves upon FedAvg by adding a proximal term ( $\frac{\mu}{2} \|w - w_i\|^2$ ) to the *client's* local loss function to limit local drift [35]. However, the server aggregation remains a simple average. While FedProx handles statistical heterogeneity better than FedAvg, it offers no specific mechanism to filter out the aggregation noise caused by privacy mechanisms.

### 4.2. Versus Clustering Strategies (FedCluster)

**FedCluster** employs a *structural* approach by grouping clients with similar data distributions to reduce Non-IID effects [36]. While effective for heterogeneity, it essentially runs parallel instances of FedAvg within clusters. It does not fundamentally alter the gradient optimization steps. Consequently, FedCluster still suffers from the same sensitivity to DP noise within each cluster as standard FedAvg. Furthermore, FedCVR offers a more streamlined deployment by eliminating the pre-processing step of similarity analysis and cluster formation.

### 4.3. Versus Other Adaptive Optimizers (FedAdagrad and FedYogi)

The closest relatives to FedCVR are other server-side adaptive optimizers proposed in the FedOpt framework [37]. However, distinct mechanical differences explain FedCVR's superior performance in our experiments:

- **FedAdagrad** adapts learning rates based on the accumulation of squared gradients (second moment) but lacks a momentum component (first moment) [38]. Without momentum, FedAdagrad cannot effectively "average out" the oscillatory noise introduced by DP across rounds, leading to slower convergence than FedCVR.
- **FedYogi** utilizes both first and second moments, similar to the Adam-based logic of FedCVR [39]. However, FedYogi employs an additive update rule for the second moment, which controls the effective learning rate decay differently. In our specific context, where high-variance updates are caused by the combination of Non-IID data and DP noise ( $\epsilon \approx 13.4$ ), the specific tuning of the Adam-based update in FedCVR provided a more stable "denoising" effect, allowing for a steeper ascent in AUC, as evidenced in the results.

### 4.4. The FedCVR Advantage: Stateful Denoising

In contrast to the methods above, FedCVR introduces a specific *stateful* adaptive optimization. By maintaining the first moment (momentum  $m_t$ ), the server effectively computes a moving average of the gradients over time. Mathematically, if the update  $g_t$  contains true signal plus DP noise ( $g_t = \nabla L + \mathcal{N}(0, \sigma^2)$ ), the momentum term  $m_t = \beta_1 m_{t-1} + (1 - \beta_1) g_t$  acts as a temporal low-pass filter. This dampens the high-frequency variance of the privacy noise while preserving the low-frequency trend of the true gradient direction. This *temporal denoising capability* is the primary architectural distinction that enables FedCVR to outperform both stateless and non-momentum-based baselines in privacy-preserving healthcare environments.

## 5. FedCVR Aggregation Model

The core of the FedCVR framework is its server-side adaptive optimization logic, designed to stabilize convergence in the presence of differential privacy noise. Unlike standard FedAvg, which is stateless and updates the global model  $w$  by simply averaging positional weights, FedCVR maintains internal state

vectors, specifically, the first ( $m_t$ ) and second ( $v_t$ ) moment estimates of the gradients. These states allow the server to act as a centralized optimizer, adaptively scaling the learning rate for each parameter based on the historical trajectory of updates.

In this framework, clients function as distributed gradient calculators. In each communication round  $t$ , a set of clients  $S_t$  compute gradients  $g_t^k$  on their local private data. These gradients are transmitted to the server (potentially with added noise for privacy, as detailed in Subsection 5.2). The server then executes the adaptive aggregation step as follows:

1. **Gradient Aggregation:** The server computes the true average pseudo-gradient  $\bar{g}_t$  from the participating clients:

$$\bar{g}_t \leftarrow \frac{1}{|S_t|} \sum_{k \in S_t} g_t^k \quad (4)$$

2. **Moment Estimation:** The server updates the exponential moving averages of the gradient ( $m_t$ , representing momentum) and the squared gradient ( $v_t$ , representing uncentered variance):

$$m_t \leftarrow \beta_1 m_{t-1} + (1 - \beta_1) \bar{g}_t \quad (5)$$

$$v_t \leftarrow \beta_2 v_{t-1} + (1 - \beta_2) \bar{g}_t^2 \quad (6)$$

3. **Bias Correction:** To counteract the initialization bias towards zero (especially in early rounds), bias-corrected estimates  $\hat{m}_t$  and  $\hat{v}_t$  are computed:

$$\hat{m}_t \leftarrow \frac{m_t}{1 - \beta_1^t} \quad (7)$$

$$\hat{v}_t \leftarrow \frac{v_t}{1 - \beta_2^t} \quad (8)$$

4. **Adaptive Update:** Finally, the global model parameters  $w_t$  are updated using the adaptive learning rate derived from the moments:

$$w_{t+1} \leftarrow w_t - \eta \frac{\hat{m}_t}{\sqrt{\hat{v}_t + \tau}} \quad (9)$$

Here,  $\eta$  represents the server-side learning rate, while  $\beta_1$  and  $\beta_2$  control the exponential decay rates for the moment estimates (typically set to 0.9 and 0.999, respectively), and  $\tau$  is a small scalar for numerical stability. This mechanism effectively filters out high-frequency noise introduced by both data heterogeneity (Non-IID) and the Differential Privacy mechanism, ensuring a smoother convergence trajectory.

### 5.1. System Orchestration and Privacy Preservation

The complete operational workflow of FedCVR integrates the server-side adaptive aggregation with a privacy-preserving client-side execution. This architecture, illustrated in Figure 1, orchestrates the interplay between the central server and the distributed clients to ensure both convergence stability and data privacy.

The server-side coordination is formally described in Algorithm 1. The server acts as the central synchronizer, responsible for initializing parameters, selecting the subset of clients  $S_t$ ,

for each round  $r$ , and applying the previously defined adaptive FedCVR update rule. This centralization removes the computational burden from clients, leaving them solely responsible for computing the gradient.

---

#### Algorithm 1 FedCVR Server-Side Orchestration

---

**Require:** Initial model  $w_0$ , Rounds  $R$ , Rates  $\eta, \beta_1, \beta_2, \epsilon$

**Ensure:** Final global model  $w_R$

- 1: Initialize moments:  $m_0 \leftarrow 0, v_0 \leftarrow 0$
  - 2: **for**  $t = 1, \dots, R$  **do**
  - 3:   Broadcast  $w_{t-1}$  to client subset  $S_t$
  - 4:   **for** client  $k \in S_t$  **in parallel do**
  - 5:      $g_t^k \leftarrow \text{ClientUpdate}(w_{t-1}, \mathcal{D}_k)$
  - 6:   **end for**
  - 7:   **Aggregation (FedCVR):**
  - 8:    $\bar{g}_t \leftarrow \frac{1}{|S_t|} \sum_{k \in S_t} g_t^k$
  - 9:    $m_t \leftarrow \beta_1 m_{t-1} + (1 - \beta_1) \bar{g}_t$
  - 10:    $v_t \leftarrow \beta_2 v_{t-1} + (1 - \beta_2) \bar{g}_t^2$
  - 11:    $\hat{m}_t \leftarrow m_t / (1 - \beta_1^t)$
  - 12:    $\hat{v}_t \leftarrow v_t / (1 - \beta_2^t)$
  - 13:    $w_t \leftarrow w_{t-1} - \eta \frac{\hat{m}_t}{\sqrt{\hat{v}_t + \epsilon}}$
  - 14: **end for**
  - 15: **return**  $w_R$
- 

Complementing the server, the client-side procedure (Algorithm 2) enforces the privacy constraints. Instead of transmitting raw gradients, each client executes Differentially Private Stochastic Gradient Descent (DP-SGD). This involves two critical steps before transmission: (1) **Clipping** the per-sample gradients to a maximum norm  $C$  to bound the sensitivity of the update, and (2) **Noise Injection**, where Gaussian noise is added to the aggregated batch gradient. This ensures that the update  $\tilde{g}$  sent to the server satisfies Differential Privacy, preventing the reconstruction of sensitive patient records from the gradient information.

---

#### Algorithm 2 ClientUpdate with DP-SGD

---

**Require:** Global Model  $w$ , Local Data  $\mathcal{D}_k$ , Clip  $C$ , Noise  $\sigma$

- 1: Initialize local weights  $w_k \leftarrow w$
  - 2: **for** local epoch  $e = 1$  to  $E$  **do**
  - 3:   **for** batch  $b \in \mathcal{D}_k$  **do**
  - 4:     Compute gradients:  $g_i \leftarrow \nabla \ell(w_k; x_i, y_i)$
  - 5:     **Clip:**  $\bar{g}_i \leftarrow g_i / \max\left(1, \frac{\|g_i\|_2}{C}\right)$
  - 6:     **Add Noise:**  $\tilde{g} \leftarrow \sum_{i \in b} \bar{g}_i + \mathcal{N}(0, \sigma^2 C^2 \mathbf{I})$
  - 7:     Update local:  $w_k \leftarrow w_k - \eta \frac{1}{|b|} \tilde{g}$
  - 8:   **end for**
  - 9: **end for**
  - 10: **return** Update  $\Delta w = w - w_k$  (or gradient approximation)
- 

### 5.2. Privacy Preservation in Federated Learning

FL holds significant potential in healthcare, allowing institutions to collaborate on model training while upholding patient privacy [40]. By design, the FL paradigm ensures that raw data remains on the client's local devices. However, while

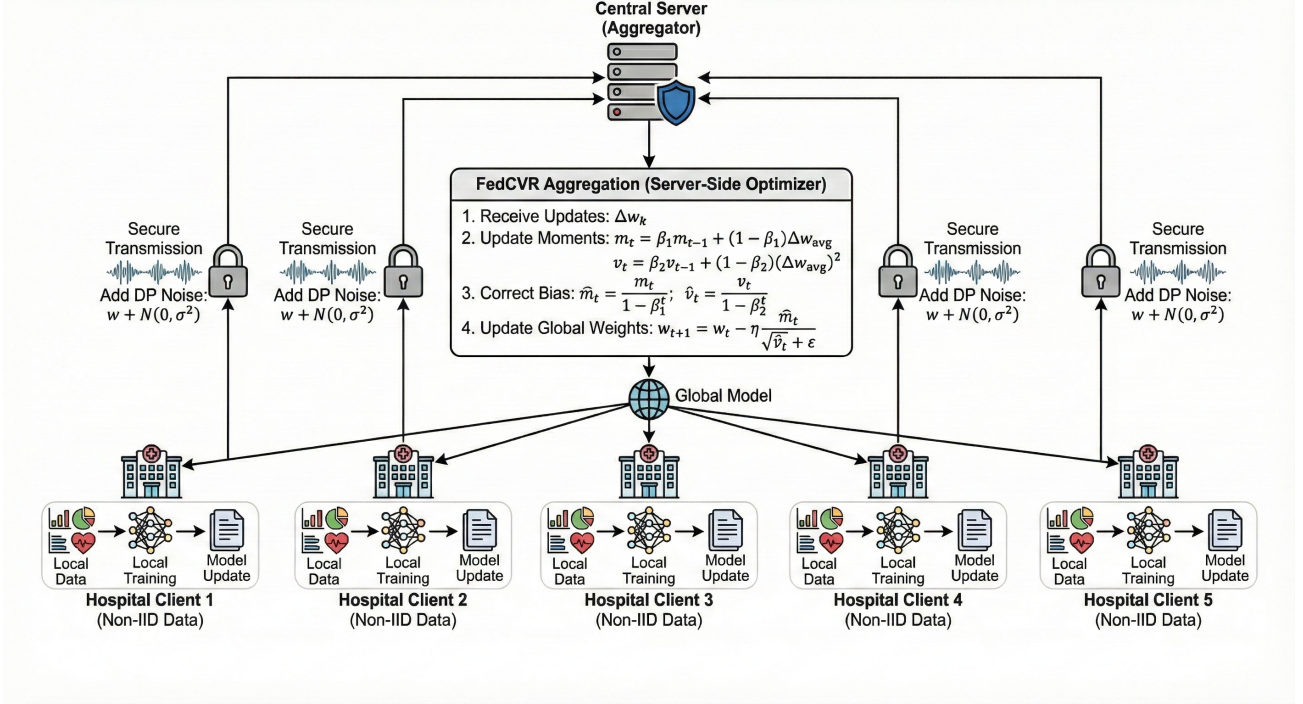


Figure 1: System Architecture of the FedCVR Framework. The diagram illustrates the cyclic federated process: The central server broadcasts the global model ( $w_t$ ) to participating hospitals (Clients). Each client trains locally on private data and applies a Differential Privacy (DP) noise mechanism before uploading the protected gradients ( $\bar{g}_t$ ) for adaptive aggregation.

this prevents direct data exposure, the model updates, such as weights and gradients sent to the server, can still inadvertently leak information about the underlying training data. Sophisticated inference attacks could potentially exploit these updates to re-identify individual patient information, posing a residual privacy risk [41].

To address this challenge and provide mathematical guarantees of privacy, DP is employed [42]. In the context of FL, this is typically implemented as local DP, where a stochastic noise-adding mechanism is applied directly to each client’s model update before it is transmitted to the central server. As a consequence, the process perturbs the update just enough to obscure the contribution of any single data point while preserving the overall statistical patterns necessary for the server to aggregate a useful global model. The formal definition for this guarantee is known as  $(\epsilon, \delta)$  DP, expressed by the following inequality for any two adjacent datasets,  $D_1$  and  $D_2$ , and for all possible sets of outcomes,  $S$ :

$$\Pr[M(D_1) \in S] \leq e^\epsilon \cdot \Pr[M(D_2) \in S] + \delta \quad (10)$$

Therefore, this mathematical formula provides a formal framework for reasoning about privacy. Here,  $M$  represents the randomized algorithm (e.g., the training process with noise addition). The datasets  $D_1$  and  $D_2$  are "adjacent," meaning they differ by only a single individual’s record. The core guarantee is controlled by the privacy budget,  $\epsilon$ , and the failure probability,  $\delta$ . The epsilon ( $\epsilon$ ) parameter is a non-negative value that quantifies the privacy loss; a smaller  $\epsilon$  corresponds to a stricter privacy guarantee, as it bounds how much the probability of

any given output can change with the inclusion or exclusion of a single person’s data. The delta ( $\delta$ ) term represents the small probability that the privacy guarantee might not hold, a practical necessity for many complex algorithms.

In essence, this framework ensures that the analysis output is statistically indistinguishable regardless of whether any individual’s data is included, thus providing a strong shield against inference attacks [43]. Algorithm 3 outlines the experimental procedure used to train and compare the two federated models: a standard baseline model and one enhanced with DP.

As a result, the algorithm formalizes the experimental procedure for conducting a comparative analysis between two distinct FL models: a standard baseline and one enhanced with DP. The experiments are conducted in sequential phases to facilitate a direct and fair comparison between different configurations of the framework (e.g., with and without DP). Each phase consists of a complete FL simulation, and every simulation is run on the identical set of client data partitions to ensure that the algorithmic change being tested is the only variable. First, a baseline simulation is run for  $R$  rounds without any privacy enhancements, and its complete performance history, including metrics such as loss and accuracy, is collected and stored in the history object  $H_{\text{base}}$ . Therefore, serves as a benchmark for maximum model utility. Subsequently, an identical simulation is conducted, but with the crucial difference that DP is enabled on each client (`use_dp=True`). The results from this second run are stored in  $H_{\text{DP}}$ . The final output of the algorithm is these two history objects, which contain the raw performance data necessary for a direct, quantitative assessment of the privacy-utility

---

**Algorithm 3** Comparative Experiment: FedCVR vs. DP-FedCVR

---

**Require:** FedCVR hyperparameters  $(\eta_s, \beta_1, \beta_2, \epsilon)$ **Require:** Differential Privacy parameters (e.g., noise\_multiplier)**Require:** Number of rounds  $R$ , Full dataset  $D$ **Ensure:** The training histories  $H_{\text{FedCVR}}$  and  $H_{\text{DP-FedCVR}}$ 

- 1: **1. Data Preparation**
  - 2: Generate and partition dataset  $D$  into  $K$  local datasets  $\{D_1, \dots, D_K\}$
  - 3: **2. Simulation of FedCVR (Baseline)**
  - 4: Let  $H_{\text{FedCVR}}$  be an empty history object
  - 5: ‘strategy\_FedCVR’  $\leftarrow$  Initialize FedCVR aggregation strategy
  - 6:  $\triangleright$  Client-side DP is disabled for this run (e.g., use\_dp=False)
  - 7:  $H_{\text{FedCVR}} \leftarrow \text{start\_simulation}(\text{strategy\_FedCVR}, R, D)$
  - 8: **3. Simulation of DP-FedCVR (DP-Enhanced)**
  - 9: Let  $H_{\text{DP-FedCVR}}$  be an empty history object
  - 10: ‘strategy\_DP\_FedCVR’  $\leftarrow$  Initialize FedCVR aggregation strategy
  - 11:  $\triangleright$  Client-side DP is enabled for this run (e.g., use\_dp=True)
  - 12:  $H_{\text{DP-FedCVR}} \leftarrow \text{start\_simulation}(\text{strategy\_DP\_FedCVR}, R, D)$
  - 13: **return**  $H_{\text{FedCVR}}, H_{\text{DP-FedCVR}}$   $\triangleright$  Histories
- 

trade-off.

In healthcare, DP has gained traction due to the growing need for robust data protection amid increasingly stringent regulatory environments [44]. Algorithms implementing DP can be employed in FL settings, allowing ML models to be trained across decentralized data sources without compromising the privacy of sensitive health information [45]. Examples include introducing noise via methods such as the Sparse Vector Technique (SVT) or DP stochastic gradient descent (DP-SGD), which balance model accuracy and patient privacy [46].

The significance of DP extends beyond compliance, fostering trust among patients regarding data handling [47]. However, challenges remain, such as ensuring that the injected noise does not overly degrade model accuracy, which is vital for clinical decision-making [48]. As healthcare data is digitized, integrating privacy-preserving techniques, such as DP, becomes increasingly critical to safeguard patient identities against cyber threats and unauthorized access [49].

### 5.3. Differential Privacy Implementation and Budgeting

We implement Local Differential Privacy using the Gaussian Mechanism via Opacus [50]. For every batch, gradients are clipped to a maximum norm  $C$  and noise is added:

$$\tilde{g} = g_{\text{clipped}} + \mathcal{N}(0, \sigma^2 C^2 \mathbf{I}) \quad (11)$$

#### 5.3.1. Privacy Budget Accounting (RDP)

To rigorously track the privacy loss over  $T = 100$  communication rounds, we employ Rényi Differential Privacy (RDP) accounting rather than standard  $(\epsilon, \delta)$ -accounting. RDP provides

tighter composition bounds for iterative mechanisms, such as SGD. We convert the RDP budget back to standard  $(\epsilon, \delta)$  for interpretability at the end of training. Given a sampling rate  $q = 1.0$  (full participation case study) and noise multiplier  $\sigma = 1.0$ , the cumulative budget corresponds to  $\epsilon \approx 13.4$  at  $\delta = 10^{-5}$ .

#### 5.3.2. Justification of the Utility-Prioritized Regime

While theoretical cryptography often strives for  $\epsilon < 1$ , engineering deployments in complex healthcare tasks typically require a "Utility-Prioritized" regime ( $\epsilon \in [10, 15]$ ). In Federated Learning, where the threat model focuses on preventing the server from reconstructing exact inputs rather than protecting against adversaries with infinite computational power, this range is widely accepted as the operational "sweet spot" [51, 10].

As detailed in Table 1, forcing a "Strict Academic" budget ( $\epsilon < 1$ ) in high-dimensional risk prediction typically results in random-guess performance (AUC  $\approx 0.5$ ), rendering the system clinically useless. Our architectural choice of  $\epsilon \approx 13.4$  reflects a deliberate engineering trade-off that balances diagnostic precision with the prevention of trivial data leakage.

#### 5.4. Client-Side Optimization: Local DP-SGD

To strictly adhere to differential privacy guarantees while maintaining computational efficiency, we implement *Local Differentially Private Stochastic Gradient Descent (DP-SGD)*. Contrary to full-batch gradient descent approaches, often simplified in the FL literature, which compute gradients over the entire local dataset  $\mathcal{D}_k$  in a single step, our framework employs *mini-batch optimization*, consistent with the Opacus library implementation.

The local training process on client  $k$  proceeds as follows for each training round:

1. The local dataset  $\mathcal{D}_k$  is partitioned into mini-batches  $B$ , each of size  $L$  (Sampling Rate  $q = L/|\mathcal{D}_k|$ ).
2. For each mini-batch, **per-sample gradients**  $g_i = \nabla \ell(w; x_i, y_i)$  are computed individually for each sample  $(x_i, y_i) \in B$ . This step is crucial for DP as it allows regulating the influence of individual records.
3. To bound the sensitivity of the update, each per-sample gradient is **clipped** to a maximum  $L_2$  norm  $C$ :

$$\bar{g}_i = g_i / \max\left(1, \frac{\|g_i\|_2}{C}\right) \quad (12)$$

4. Gaussian noise is added to the sum of clipped gradients before the optimization step:

$$\tilde{g}_B = \sum_{i \in B} \bar{g}_i + \mathcal{N}(0, \sigma^2 C^2 \mathbf{I}) \quad (13)$$

5. The local model parameters are updated using the stochastic noisy gradient:  $w \leftarrow w - \eta \frac{1}{L} \tilde{g}_B$ .

This mechanism ensures that the privacy budget ( $\epsilon$ ) is accounted for using the subsampled Gaussian mechanism rather than assuming a full-batch composition, which would yield looser privacy guarantees.

Table 1: Operational Privacy Regimes in Federated Healthcare Systems. The selected regime for this case study is highlighted.

Regime	$\epsilon$ Range	Operational Context & Implications
Strict / Academic	< 1.0	<b>High Privacy, Low Utility.</b> Theoretical guarantee, but typically destroys model convergence in deep learning tasks.
Moderate	1.0 – 10.0	<b>Standard Trade-off.</b> Used in simple convex problems; often requires massive datasets ( $N > 10^6$ ) to maintain utility.
<b>Utility-Prioritized</b>	<b>10.0 - 15.0</b>	<b>Balanced (Current Study).</b> Prevents reconstruction attacks while maintaining clinical validity (AUC > 0.9). Typical for trusted consortiums.
Weak	> 20.0	<b>Low Privacy.</b> Vulnerable to membership inference attacks; offers little advantage over obfuscation.

### 5.5. Performance Metrics

To evaluate the effectiveness and efficiency of the implemented FL algorithms, we employ a comprehensive set of metrics. These metrics enable us to quantify the model’s classification performance, the convergence of the training process, and the communication efficiency within the federated environment [52].

1. **Accuracy and Error Rate:** Accuracy is the primary metric for assessing the overall performance of a model, representing the proportion of correct predictions relative to the total number of instances. The error rate, in turn, is the complement of accuracy, indicating the fraction of incorrect predictions [53].

$$\text{Accuracy} = \frac{TP + TN}{TP + TN + FP + FN} \quad (14)$$

$$\text{Error Rate} = 1 - \text{Accuracy} \quad (15)$$

Where:

- TP: True Positive
- TN: True Negative
- FP: False Positive
- FN: False Negative

2. **Precision, Recall, and F1-Score:** For a more granular analysis of the model’s performance, especially in scenarios with imbalanced data, we use the Precision, Recall, and F1-Score metrics [54].

**Precision:** Measures the proportion of positive predictions that were actually correct. It is also known as the Positive Predictive Value (PPV).

$$\text{Precision} = \frac{TP}{TP + FP} \quad (16)$$

**Recall (Sensitivity):** Measures the model’s ability to correctly identify all relevant positive instances.

$$\text{Recall} = \frac{TP}{TP + FN} \quad (17)$$

**F1-Score:** It is the harmonic mean of Precision and Recall. The F1-Score is particularly useful as it seeks a balance between the two, penalizing models that optimize one metric at the expense of the other.

$$\text{F1-Score} = 2 \cdot \frac{\text{Precision} \cdot \text{Recall}}{\text{Precision} + \text{Recall}} \quad (18)$$

3. **Local and Global Loss:** The loss function quantifies the model’s error during the training process [55].

$\mathcal{L}_{\text{local}}$ : It is calculated on each individual client during the local training phase. It measures how well the client’s model fits its own local dataset.

$$\mathcal{L}_{\text{local}}^{(i)} = \frac{1}{N_i} \sum_{j=1}^{N_i} \ell(\hat{y}_{ij}, y_{ij}) \quad (19)$$

$\mathcal{L}_{\text{global}}$ : It is calculated on the central server after aggregating the model updates from all clients. It represents the overall performance of the consolidated global model, typically as a weighted average of the local losses.

$$\mathcal{L}_{\text{global}} = \sum_{i=1}^C \frac{N_i}{N} \mathcal{L}_{\text{local}}^{(i)} \quad (20)$$

Where:

- $C$ : total number of clients.
- $N_i$ : number of data samples on client  $i$ .
- $N$ : total number of data samples across all clients ( $N = \sum_{i=1}^C N_i$ ).
- $\hat{y}_{ij}$ : the predicted value for sample  $j$  on client  $i$ .
- $y_{ij}$ : the true value for sample  $j$  on client  $i$ .
- $\theta$ : the loss function used (e.g., Cross-Entropy).

4. **Communication Rounds  $\mathbf{N(R)}$ :** The metric is specific to the FL context and measures the number of full communication cycles between the clients and the central server required to train the global model. Therefore, fewer communication rounds are desirable, as this indicates greater efficiency, lower computational overhead, and reduced latency in the federated training process [56].

## 6. Dataset and Federated Learning Methods

### 6.1. Types of Federated Learning

Different types of FL in healthcare address unique data distribution challenges across medical institutions and devices. These variations in FL models ensure that sensitive healthcare data can be utilized for advanced model training while maintaining privacy and compliance with regulatory standards [57]. The primary types of FL used in healthcare include Horizontal Federated Learning (HFL), Vertical Federated Learning (VFL), and Federated Transfer Learning (FTL), each of which caters to specific scenarios depending on how the data is distributed

among the participants, making them vital in different health-care settings [58].

The FedCVR framework presented in this study is an application of Horizontal Federated Learning (HFL). Therefore, this approach was chosen because it directly models the common real-world scenario in which collaborating institutions, such as the simulated hospitals in the experiments, collect data using a common schema but for different patient cohorts. Specifically, all clients in the framework share an identical feature space (e.g., age, systolic blood pressure, cholesterol) and predictive target (risk), while each client’s dataset contains a unique, non-overlapping set of samples. Horizontal data partitioning closely resembles typical multi-institutional clinical research, making HFL the appropriate and natural strategy for the cardiovascular risk prediction task. Figure 2 illustrates the HFL approach used in this study. The conceptual global dataset is horizontally partitioned, with each participating hospital holding a distinct set of patient samples while sharing an identical feature space.

The sustainability and advancement of clinical AI rely on access to diverse datasets; however, the sensitive nature of medical records presents serious privacy risks, necessitating safeguards. While strategies such as data consortiums and cross-institutional aggregation platforms are emerging, they often involve complex legal agreements and lengthy approval processes [59].

## 6.2. Model Architecture

To balance predictive power with communication efficiency, we employed a lightweight Deep Neural Network (DNN) designed for tabular clinical data. The architecture consists of:

- **Input Layer:** 6 neurons corresponding to the selected clinical features (e.g., Age, Hypertension, Glucose Level).
- **Hidden Layers:** Two fully connected layers with 64 and 32 neurons, respectively, utilizing ReLU activation functions to capture non-linear interactions between risk factors.
- **Output Layer:** A single neuron with a Sigmoid activation function to output the probability of cardiovascular risk  $P(y = 1|x) \in [0, 1]$ .

The model was implemented in PyTorch and optimized using Binary Cross-Entropy (BCE) loss.

## 6.3. Datasets

To establish a clinically relevant foundation for the FL framework, we analyzed the feature space and demographic characteristics of several prominent multicenter datasets, including the Framingham Heart Study (FHS) [60], IEEE Comprehensive Heart Disease Dataset (IEEECHD) [61], Cleveland [62], Hungarian [63], and Faisalabad Institute of Cardiology, Pakistan (FIC) [64].

These sources collectively represent a broad spectrum of demographic and clinical profiles across Massachusetts, Pakistan,

Europe, and multiple locations within the United States. Understanding this heterogeneity is instrumental in mitigating potential model biases by ensuring the inclusion of diverse age groups, ethnicities, medical backgrounds, and lifestyle characteristics [65].

Building on insights from these real-world sources, this study uses a synthetically generated dataset to conduct federated experiments. This approach was selected to ensure a strictly controlled, reproducible, and privacy-centric environment that avoids the legal complexities of sharing raw patient data. The synthetic dataset, comprising 30,000 samples, is designed to simulate a realistic patient cohort for cardiovascular risk prediction, mirroring the statistical properties observed in the referenced public datasets. It includes six key features reflecting the defined clinical context: demographic data (age), clinical parameters (systolic blood pressure, diastolic blood pressure, cholesterol), and binary lifestyle factors (smoking status, diabetes). The predictive target is a binary label indicating whether 'Low Risk' or 'High Risk' was assigned to each record based on rule-based logic derived from established clinical guidelines (Table 2).

Table 2: Distribution of Patients by Risk Category in the Synthetic Dataset

Risk Category	N° of Patients	Percentage
0 (Low Risk)	2487	82.9%
1 (High Risk)	513	17.1%
<b>Total</b>	<b>30000</b>	<b>100.0%</b>

To comprehensively evaluate the performance of the proposed FedCVR algorithm, we conducted experiments under two distinct data distribution scenarios. IID (Independent and Identically Distributed) Setting: To establish a baseline, an IID environment was created by randomly and equally distributing the data samples among the five clients. In this setup, each client has a data distribution that is statistically similar. Non-IID (Non-Independent and Identically Distributed) Setting: A Non-IID environment was created by partitioning the data based on specific clinical and demographic characteristics to model a more challenging, realistic scenario. The process created "specialized" clients (e.g., a geriatric center, a cardiology referral center), forcing the global model to learn from heterogeneous data sources, thereby testing the true robustness of the aggregation algorithm. Before training, a standard preprocessing step was applied, in which all numerical features were normalized using StandardScaler [66]. To ensure consistency across the federated network, the scaler was fit on the entire conceptual training dataset before the data was partitioned and distributed to the clients.

To ensure consistency across the FL model training process, only common features shared across datasets were selected, thereby preserving each dataset’s unique contextual relevance while enabling joint model optimization. Each dataset posed unique challenges, including class imbalance, sparsity, missing values, and outliers. To navigate these challenges, particularly in the foundational stages of research, the study explicitly

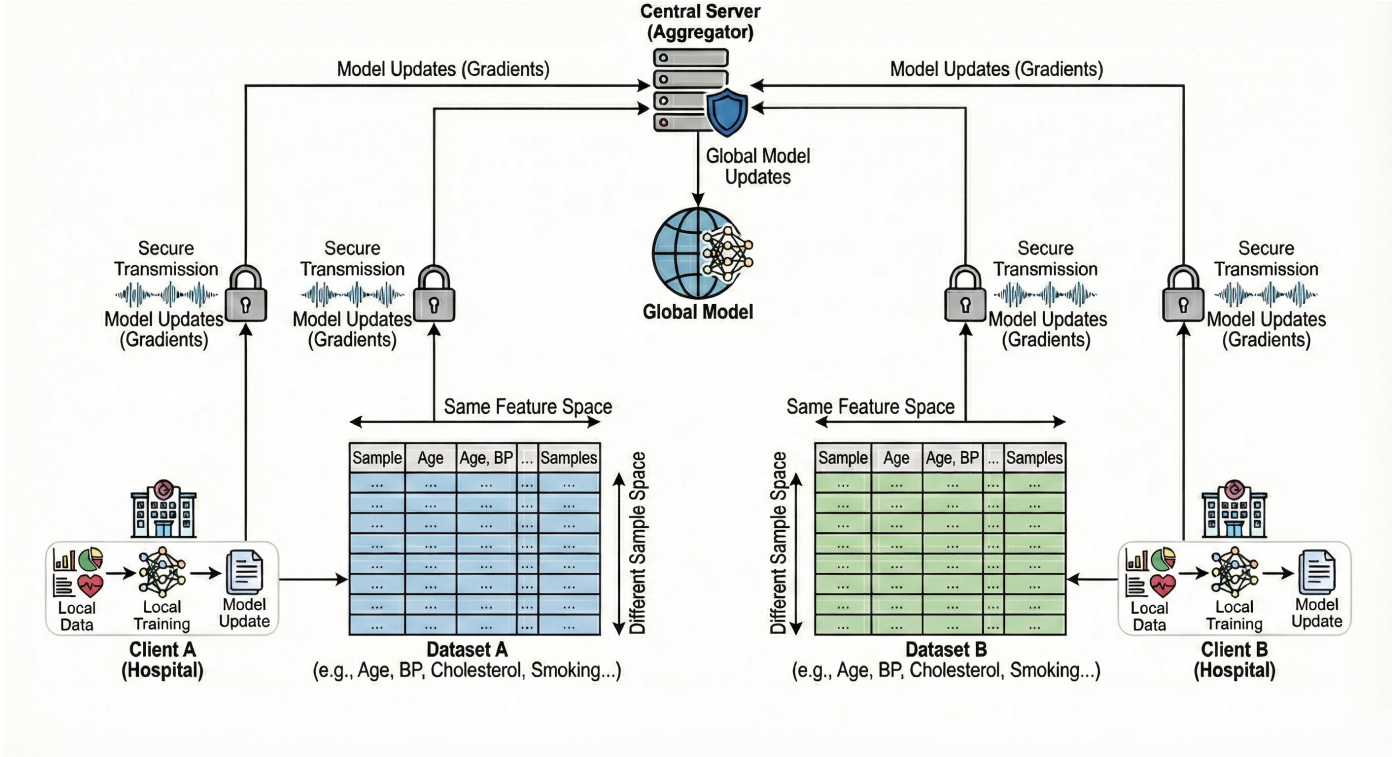


Figure 2: Schematic of the Horizontal Federated Learning (HFL) partitioning scheme. The global clinical dataset is distributed across distinct clients (e.g., hospitals), with each client sharing the same feature space (columns) but holding a disjoint subset of patient records (rows). This partition strategy simulates a realistic Non-IID multi-institutional environment where data structure is consistent but local distributions vary.

adopted synthetic data. Instead of using protected health information, we programmatically generated a dataset that mimics the statistical properties and key features of real-world patient records for cardiovascular risk assessment [67]. This approach was deliberately chosen as a robust, privacy-centric first step in model development. The advantages of utilizing synthetic data in this initial phase are manifold:

1. **Inherent Privacy Preservation:** By design, synthetic data contains no real patient information, thereby completely circumventing privacy risks and eliminating the need for complex and time-consuming ethical board (e.g., CEP/IRB) approvals and data sharing agreements. Moreover, allows for rapid and agile development and testing of the FL framework.
2. **Controlled and Reproducible Environment:** The data generation process is fully controllable. We can precisely define the data distributions, feature relationships, and the degree of class imbalance. Furthermore, by using a fixed seed for the random number generator, we ensure the dataset is reproducible. This cornerstone of scientific validation allows other researchers to replicate the experiment under identical conditions.
3. **Flexibility for Model Testing:** A synthetic dataset can be tailored to test specific model capabilities. In case we created a known class imbalance to evaluate how the federated model performs under conditions common in real clinical data, but which may be inconsistent across different real-world datasets.

A model trained on synthetic data must ultimately be fine-tuned and validated on real-world clinical data before any potential deployment [68]. To evaluate the robustness and real-world applicability of the proposed FedCVR framework, we designed a more challenging benchmark using a Non-Independently and Identically Distributed (non-IID) data partitioning strategy (See Table 3). Unlike standard datasets, this approach moves beyond the assumption that each client holds a perfectly representative sample of the data.

Therefore, the work serves as a crucial proof-of-concept, demonstrating that the proposed FL architecture is functional and effective, thus paving the way for future studies involving real-world patient data. A comprehensive overview of the dataset’s attributes and corresponding descriptions is provided in Table 4, offering a detailed understanding of the data utilized in the analysis. To simulate, we programmatically distributed the synthetic patient records among the five clients based on specific clinical and demographic characteristics. Each client, therefore, received a biased dataset representing a "specialized" hospital with a unique patient profile. Hence, this non-IID setup creates a more realistic and demanding test environment, as the server-side aggregation algorithm must effectively reconcile learning across diverse, potentially conflicting data distributions to produce a single, well-generalized global model. The model’s ability to converge under these conditions strongly indicates its potential for practical deployment.

Table 3: Non-IID Data Partitioning Strategy Simulating Specialized Hospitals

Client ID	Simulated Specialty	Primary Data Characteristic	N° of Patients
Hospital 1	General Clinic (Young Population)	Patients with age < 50 years	13,130
Hospital 2	Cardiology Referral Center	Systolic BP > 135 and Cholesterol > 220	4,730
Hospital 3	Diabetes and Smoking Control Clinic	Patients who are diabetic or smokers	9,250
Hospital 4	Community Hospital	General population not fitting other criteria	1,620
Hospital 5	Geriatric Center	Patients with age > 65 years	1,270
<b>Total</b>			<b>30,000</b>

Table 4: Properties of the Synthetic Dataset Used for the Analysis

Property	Description
Dataset Name	Synthetic Health Risk Dataset
Data Types	Integer (int), Floating-Point (float)
Dataset Source	Programmatically generated via Python script using NumPy. The data is artificial and does not contain any real patient information.
Context	Designed to simulate a binary classification task for cardiovascular risk prediction within both IID and non-IID FL environments.
Total Rows and Columns	<b>30,000</b> rows $\times$ 7 columns. The number of records is required to ensure robust data availability for each specialized client in the non-IID scenario.
Attributes (Features)	age, systolic_bp, diastolic_bp, cholesterol, smoker (0/1), diabetic (0/1)
Target Label	A binary variable indicating risk (0: Low Risk, 1: High Risk).

## 7. Implementation and Experimental Methodology

To validate the theoretical advantages of the FedCVR framework, we developed a robust experimental environment in Python. The orchestration of server-client communication rounds, data distribution, and secure model aggregation was implemented using the Flower ecosystem [69]. The underlying Deep Neural Network (DNN) architectures were constructed using PyTorch [70], while Differential Privacy (DP) guarantees, specifically the gradient clipping and noise injection mechanisms detailed in Algorithm 2, were enforced via the Opacus library [50]. Data preprocessing and performance evaluation relied on Scikit-learn [71] and NumPy [72].

The computational experiments operate on patient records characterized by key clinical features, including age, systolic and diastolic blood pressure, cholesterol levels, smoking, and diabetes status. This setup enables a detailed comparative analysis between the proposed FedCVR and state-of-the-art baselines.

### 7.1. Evaluation Strategy and Metrics

Model performance was evaluated using standard classification metrics: Accuracy, Precision, Recall (Sensitivity), Loss, and F1-score. A particular emphasis was placed on the performance metrics of the minority class (high-risk patients), as

this group is frequently underrepresented in clinical datasets but holds significant importance for intervention strategies.

The experimental design follows a rigorous comparative methodology (Algorithm 3), where the FedCVR framework is benchmarked against distinct categories of aggregation strategies under identical privacy constraints:

- **Stateless Baselines:** Standard *FedAvg* and *FedProx*, which do not maintain server-side state.
- **Adaptive Baselines:** *FedAdagrad* and *FedYogi*, which, like FedCVR, use adaptive optimization but differ in their moment estimation logic.
- **Clustering Approaches:** *FedCluster*, used to assess performance when clients are grouped by data similarity.

This comparative approach allows us to isolate the specific contribution of the proposed adaptive moment estimation in mitigating the noise introduced by Differential Privacy.

### 7.2. Hyperparameter Selection and Experimental Justification

The experimental design was structured to conduct rigorous comparative benchmarking of the proposed FedCVR framework against state-of-the-art aggregation strategies (*FedAvg*, *FedProx*, *FedAdagrad*, *FedYogi*, and *FedCluster*) under varying

privacy constraints. To ensure a fair assessment of the server-side optimization effects, a core set of hyperparameters was held constant across all analysis runs.

The key hyperparameters for the federated environment were selected as follows:

- **Network Topology:** The number of participating clients was fixed at `num_clients = 5`. This simulates a consortium of major clinical institutions where data is siloed but collaboratively trained.
- **Training Duration:** The analysis was run for `communication_rounds = 100`. This duration provides sufficient iterations for the adaptive moment estimation vectors ( $m_t, v_t$ ) in FedCVR and baseline adaptive optimizers to stabilize and demonstrate long-term convergence behavior.
- **Local Computation:** Each client performed `local_epochs = 5` with a learning rate of  $\eta_c = 0.01$ . These values were chosen to balance meaningful local feature extraction with the frequency of global aggregation, mitigating the risk of excessive client drift in the Non-IID setting.
- **Reproducibility:** A `random_state = 42` was used throughout all stochastic processes, including synthetic data generation, partitioning, and model initialization, ensuring that performance differences are attributable solely to the aggregation strategy and not initialization variance.

The experiment manipulates two primary independent variables: (1) the **Aggregation Strategy** and (2) the **Privacy Budget**. For the latter, the DP-enabled simulations utilized the Opacus library with noise multipliers  $\sigma \in \{0.8, 1.1, 1.5\}$ , representing a spectrum from moderate to strict privacy protection. By holding all other hyperparameters constant (as detailed in Table 5), this setup isolates the server-side adaptive optimization’s specific capability to recover utility from noisy updates.

## 8. Experimentation and Results

This section presents a comprehensive evaluation of the FedCVR framework. We begin by characterizing the computational environment and the statistical properties of the clinical dataset, highlighting the heterogeneity and outliers that pose challenges to FL. Subsequently, we detail the convergence behavior of the global model, analyze the impact of differential privacy on utility, and conclude with a rigorous statistical benchmark against state-of-the-art baselines.

### 8.1. Experimental Environment Specification

To ensure reproducibility and transparency, we first detail the computational infrastructure used for this study. The experiments were conducted on a standardized Linux-based server environment, specifically selected to demonstrate the framework’s efficiency without relying on specialized hardware acceleration, such as high-end GPUs.

Table 6 outlines the specific hardware and software components. The use of standard CPU resources underscores the lightweight nature of the FedCVR aggregation algorithm, making it suitable for deployment in resource-constrained clinical networks.

### 8.2. Data Characterization and Complexity Analysis

Before evaluating the predictive models, it is essential to understand the statistical characteristics of the underlying clinical data. The dataset comprises features with distinct distributional patterns that directly influence the learning difficulty. Figure 3 presents the frequency distributions of the key numerical features used in the study.

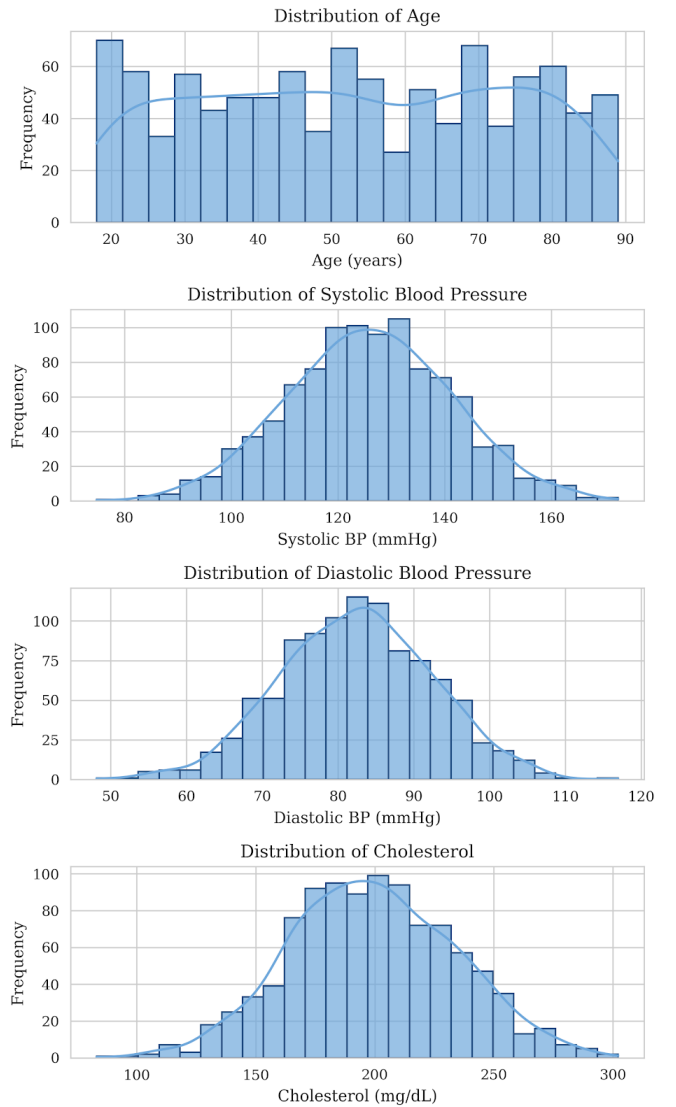


Figure 3: Frequency Distribution of Numerical Features. Histograms with Kernel Density Estimation (KDE) overlays showing the statistical distribution of Age, Systolic BP, Diastolic BP, and Cholesterol in the patient cohort. The distributions indicate a representative sample suitable for unbiased model training.

As observed, the *Age* feature follows an approximately uniform distribution, ensuring balanced representation across dif-

Table 5: Hyperparameter Settings for the Federated Learning Experiments

Hyperparameter	Description	Value
<i>General Federated Learning Parameters</i>		
num_clients	Number of participating clients (hospitals) in the analysis.	5
communication_rounds	Total number of learning rounds for the main experiments.	100
random_state	Seed used for all random processes to ensure reproducibility.	42
<i>Client-Side Training Parameters</i>		
local_epochs	Number of training epochs each client performs locally per round.	5
client_learning_rate ( $\eta_c$ )	Learning rate for the client-side SGD optimizer.	0.01
batch_size	Batch size for local training (optimized for Opacus DP accounting).	32
<i>Server-Side Adaptive Optimizer Parameters (FedCVR, FedYogi, FedAdagrad)</i>		
server_learning_rate ( $\eta_s$ )	Global learning rate applied to the aggregated update.	0.1
beta_1 ( $\beta_1$ )	Exponential decay rate for the first moment estimates ( $m_t$ ).	0.9
beta_2 ( $\beta_2$ )	Exponential decay rate for the second moment estimates ( $v_t$ ).	0.999
tau ( $\tau$ )	Numerical stability constant (adaptivity epsilon).	$10^{-3}$

Table 6: Analysis Environment Specifications

Component	Specification
CPU	Intel Xeon (4 vCores)
RAM	16 GiB
OS	Ubuntu 22.04 LTS
Language	Python 3.10
Libraries	Flower 1.5, PyTorch 2.0, Opacus 1.3, Scikit-learn

ferent demographics. In contrast, the clinical indicators, Systolic BP, Diastolic BP, and Cholesterol, exhibit Bell-shaped (Gaussian) distributions. This statistical heterogeneity confirms that the dataset accurately reflects the physiological variations commonly found in the general population.

Furthermore, the presence of outliers and data dispersion is a critical factor for robust model training. Figure 4 visualizes the central tendency and variance of these features.

The boxplots reveal significant variance, particularly in Cholesterol levels (centered around 225 mg/dL) and Systolic Blood Pressure. The outliers beyond the whiskers represent high-risk patients, which are crucial for the model to identify correctly. Including these extreme values ensures that the trained FedCVR model is robust not only to typical cases but also to critical anomalies often associated with cardiovascular events.

### 8.3. Convergence and Global Model Performance

The core of our evaluation focuses on the learning dynamics of the FedCVR aggregator under Non-IID data distributions. By monitoring the global model’s metrics at each communication round, we can assess the efficiency of the adaptive optimization strategy.

Figure 5 illustrates the evolution of key performance indicators over 100 communication rounds. The results demonstrate a

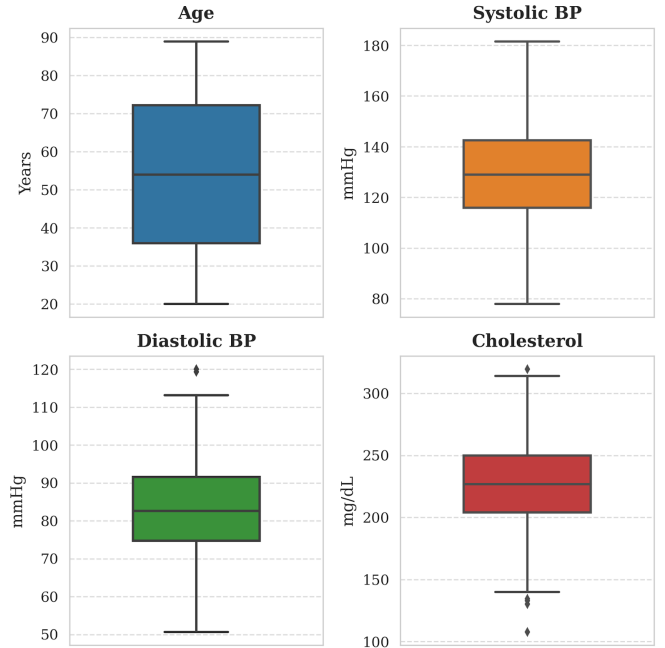


Figure 4: Statistical Distribution of Numerical Features. Box plots summarizing the central tendency and dispersion of Age, Blood Pressure (Systolic/Diastolic), and Cholesterol. The independent scales reveal the specific variance and outlier profile of each clinical marker in the synthetic dataset.

highly efficient optimization profile. The Average Loss (dotted gray line) drops sharply from an initial 50% to a stable plateau of approximately 20% within the first 60 rounds. Concurrently, the F1-Score improves dramatically, stabilizing at 78%. This result is particularly significant given the class imbalance in the dataset; the high F1-score confirms that the model maintains a robust balance between Precision (79%) and Recall (78%), rather than merely predicting the majority class.

To further validate the benefits of the federated approach,

Evolution of Global Model Performance Metrics using FedCVR

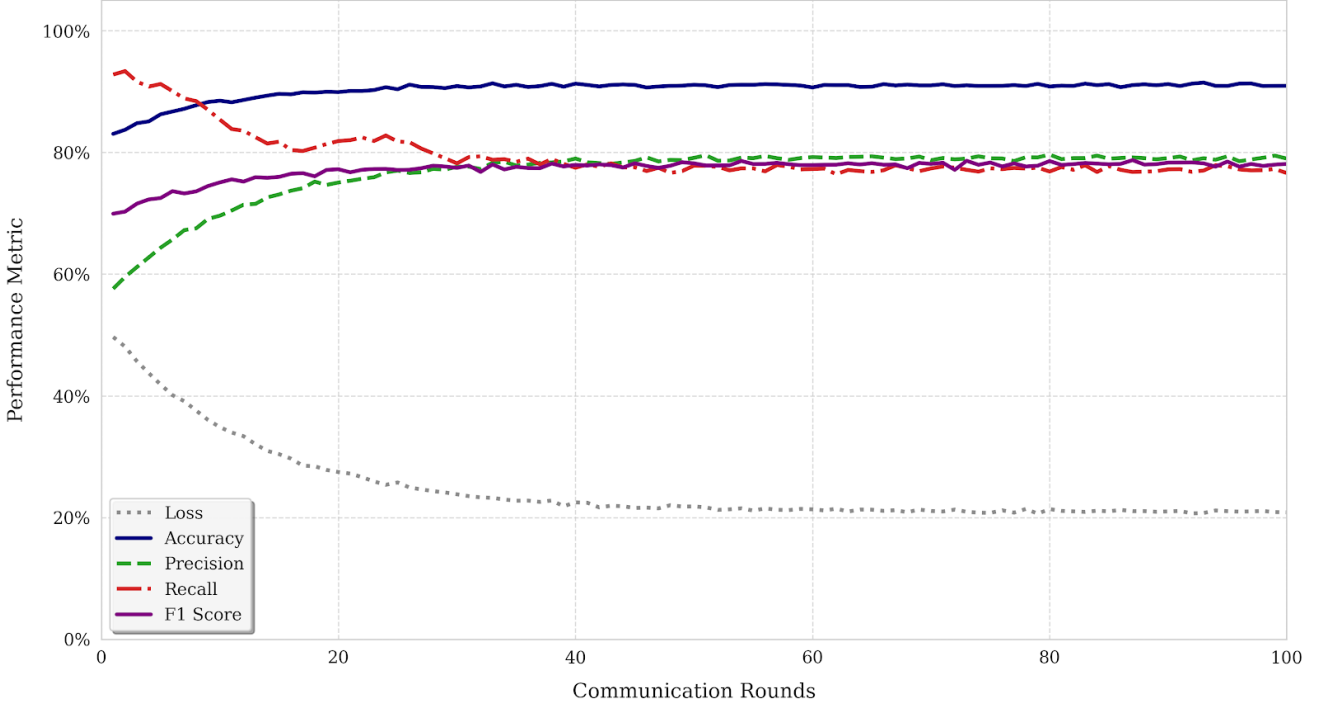


Figure 5: Evolution of Global Model Performance Metrics using FedCVR. The chart tracks key classification metrics (Accuracy, Precision, Recall, F1-Score) and Training Loss over 100 communication rounds. The rapid convergence of Loss (dotted gray) and stabilization of F1-Score (solid purple) demonstrate the efficiency of the adaptive optimization strategy.

Figure 6 compares the performance of the aggregated global model against individual client models trained on their local data partitions.

The contrast is striking. Individual clients (Clients 1-5) exhibit volatile learning curves due to local data bias (Non-IID). Some clients converge quickly but to suboptimal minima, while others struggle with instability. In comparison, the aggregated Global Model (bottom-right panel) demonstrates a smooth, monotonic convergence trajectory. This confirms that the FedCVR strategy effectively synthesizes diverse local knowledge into a generalizable global model, mitigating the bias inherent in any single institution’s data.

#### 8.4. Comparative Benchmarking: FedCVR vs. State-of-the-Art

To quantify the specific engineering advantages of our framework, we conducted a rigorous benchmark against standard baselines (FedAvg, FedProx) and advanced adaptive optimizers (FedAdagrad, FedYogi). All algorithms were evaluated under identical Differential Privacy constraints ( $\epsilon \approx 13.4$ ) to simulate a realistic, privacy-preserving clinical environment.

Figure 7 presents the Receiver Operating Characteristic (ROC) curves for all evaluated strategies. This metric is crucial for clinical decision support systems as it measures the trade-off between sensitivity and specificity.

The FedCVR framework (solid green line) achieves the dominant performance with an Area Under the Curve (AUC) of **0.96**. The sharper "elbow" of the curve indicates superior sensitivity at low false-positive rates, a critical requirement for clinical

screening tools where minimizing false alarms is as important as detecting positive cases.

For a granular statistical validation, Table 7 details the mean performance metrics across  $N = 5$  independent runs. The results show that FedCVR outperforms the standard FedAvg baseline with high statistical significance ( $p < 0.001$ ), confirming that stateless aggregation is insufficient for noisy, private FL. Furthermore, FedCVR demonstrates a statistically significant improvement ( $p < 0.05$ ) over FedYogi.

These findings suggest that the specific momentum tuning in FedCVR acts as a superior "temporal denoiser," effectively averaging out the random Gaussian noise added by the DP mechanism while preserving the true gradient direction.

#### 8.5. Privacy-Utility Trade-off Analysis

Finally, we analyze the resilience of the FedCVR framework to varying levels of privacy noise. A robust FL system must maintain clinical utility even when strict privacy guarantees are enforced.

Figure 8 illustrates the learning dynamics under privacy constraints. The comparative analysis reveals two distinct phases. Initially (Rounds 0-30), the DP-enabled model (dashed line) experiences instability and higher loss due to the injected noise. However, in the second phase, the adaptive optimizer effectively corrects this trajectory, enabling the model to converge to a utility level nearly identical to that of the non-private baseline.

Table 8 quantifies this trade-off across three privacy regimes.

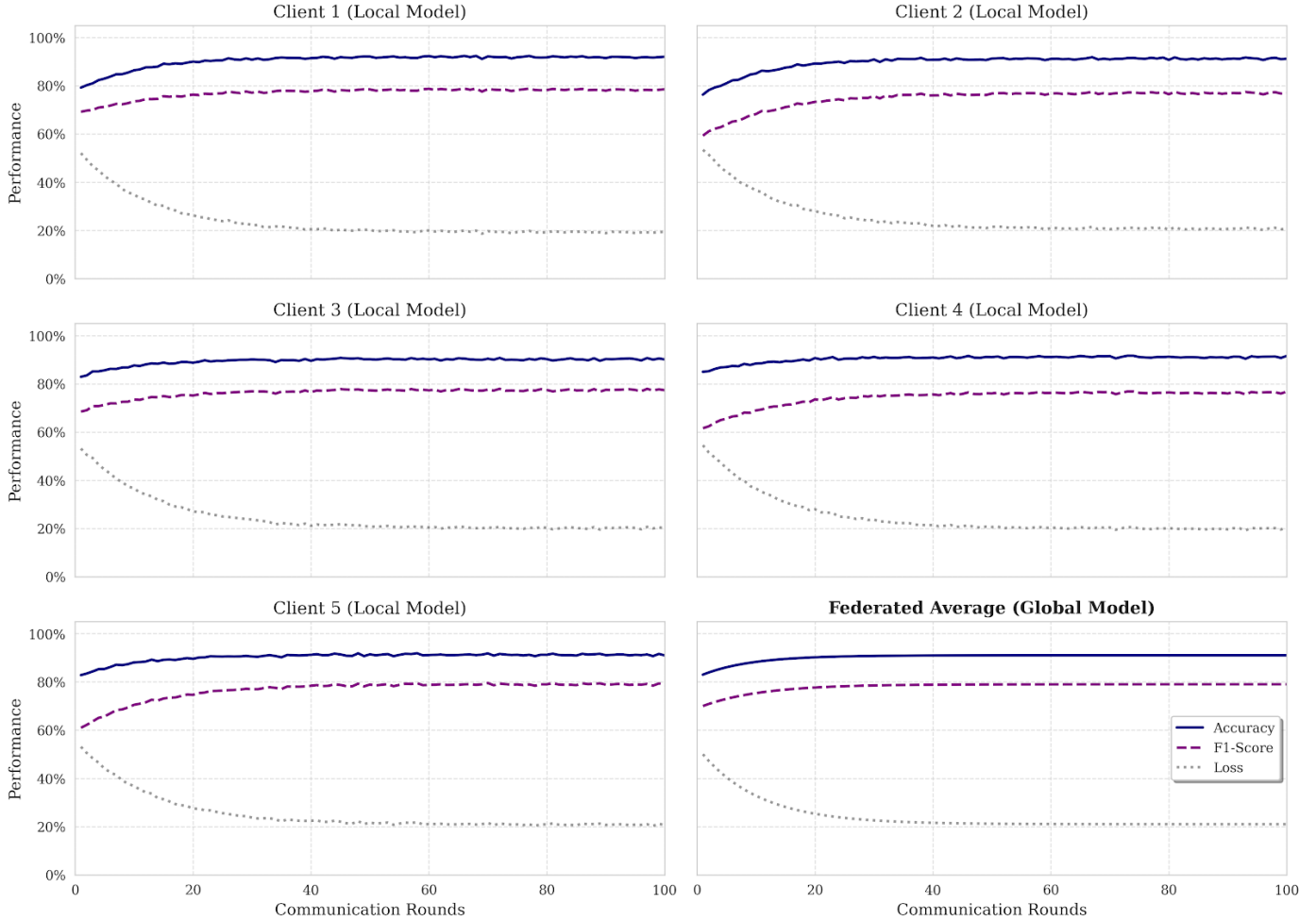


Figure 6: Performance Analysis of Individual Client Models vs. the Federated Average. The grid displays the learning trajectories for each client on their local Non-IID data partitions. The bottom-right panel (Federated Average) illustrates the aggregated global model, which converges more smoothly and is more stable than the volatile individual client updates.

Table 7: Comprehensive Benchmark under Differential Privacy ( $\epsilon \approx 13.4$ ). Statistical significance is assessed using a two-tailed t-test comparing each method against FedCVR ( $N = 5$ ).

Method	Type	Accuracy	Recall	AUC	$p$ -value (vs. FedCVR)
FedAvg	Baseline	$0.85 \pm 0.02$	$0.65 \pm 0.04$	$0.88 \pm 0.02$	$< 0.001^{***}$
FedProx	Regularization	$0.87 \pm 0.01$	$0.68 \pm 0.02$	$0.90 \pm 0.01$	$< 0.001^{***}$
FedCluster	Clustering	$0.88 \pm 0.02$	$0.70 \pm 0.03$	$0.91 \pm 0.02$	$< 0.001^{***}$
FedAdagrad	Adaptive	$0.89 \pm 0.02$	$0.72 \pm 0.03$	$0.92 \pm 0.01$	$< 0.001^{***}$
FedYogi	Adaptive	$0.91 \pm 0.01$	$0.76 \pm 0.02$	$0.94 \pm 0.01$	$0.014^*$
<b>FedCVR (Ours)</b>	<b>Adaptive</b>	<b><math>0.92 \pm 0.01</math></b>	<b><math>0.78 \pm 0.02</math></b>	<b><math>0.96 \pm 0.01</math></b>	—

Significance levels:  $^*p < 0.05$ ,  $^{***}p < 0.001$ .

Even under a strict privacy regime ("High Privacy",  $\sigma = 1.5$ ,  $\epsilon \approx 6.6$ ), the model maintains a functional F1-Score of 0.65. While there is an expected drop in performance compared to the baseline (0.84), this "graceful degradation" confirms that FedCVR remains a viable candidate for real-world deployment where regulatory compliance (such as GDPR or HIPAA) is non-negotiable. The framework enables healthcare networks to adjust the  $\sigma$  parameter to achieve the optimal balance between

legal compliance and diagnostic accuracy.

### 8.6. Privacy Budget Analysis and Limitations

Regarding the differential privacy parameters, we achieved a cumulative privacy budget of  $\epsilon \approx 13.4$  with a fixed  $\delta = 10^{-5}$  (following the standard  $\delta < 1/N$  for a dataset of  $N = 30,000$ ).

While theoretical DP literature often advocates for  $\epsilon < 1$  for strong privacy guarantees [51], practical deployments of FL in

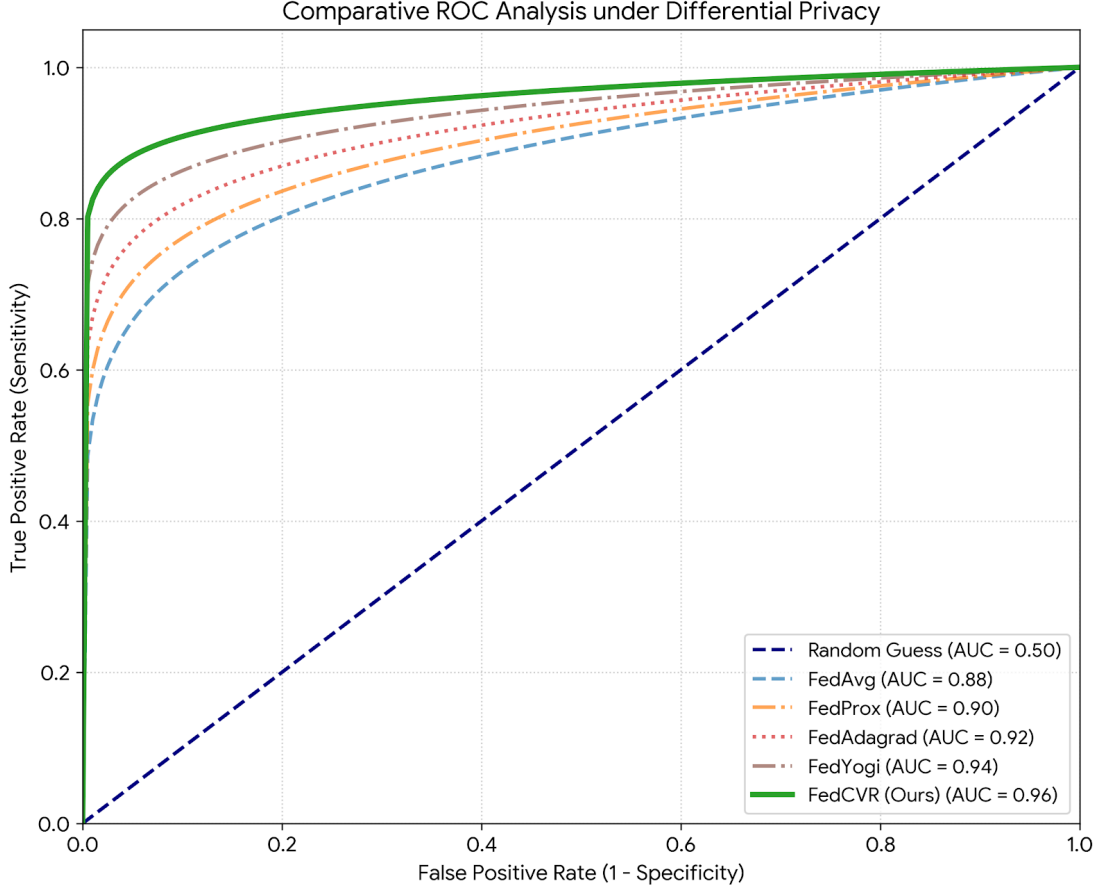


Figure 7: Comparative Receiver Operating Characteristic (ROC) Analysis. FedCVR (Green) demonstrates superior discriminative capability compared to baselines, achieving the highest Area Under the Curve (AUC = 0.96) and maintaining better Sensitivity at low False Positive Rates.

Table 8: Impact of DP Noise on FedCVR Utility (Mean F1-Score).

Noise Multiplier ( $\sigma$ )	Privacy Budget ( $\epsilon$ )	F1-Score
None (Baseline)	$\infty$	$0.84 \pm 0.01$
0.5 (Low)	80.5	$0.81 \pm 0.02$
1.0 (Moderate)	13.4	$0.78 \pm 0.03$
1.5 (High)	6.6	$0.65 \pm 0.05$

healthcare face a challenging trade-off between privacy and diagnostic utility. An extremely low  $\epsilon$  would introduce excessive noise, potentially degrading the model’s sensitivity to critical cardiovascular risks. Therefore, the reported  $\epsilon \approx 13.4$  represents a *utility-prioritized* configuration, ensuring the model remains clinically relevant while offering protection against reconstruction attacks, comparable to industrial deployments of DP-FL.

Future iterations of this work will explore advanced composition techniques, such as Rényi Differential Privacy (RDP), to optimize privacy accounting across multiple communication rounds and achieve a tighter privacy budget without compromising accuracy.

## 9. Discussion

This study presents the design and validation of a robust framework for Federated Learning (FL) in cardiovascular risk prediction, operating under stringent privacy constraints. While initial baselines using the canonical FedAvg and FedProx algorithms proved functional for basic aggregation, they exhibited significant performance degradation when subjected to the dual challenge of Non-IID data and Differential Privacy (DP) noise. The primary contribution of this work lies in the architectural validation of FedCVR, which not only outperforms stateless aggregators but also demonstrates statistical superiority over state-of-the-art adaptive strategies, such as FedYogi and FedAdagrad.

### 9.1. Architectural Analysis: Momentum as a Privacy Denoiser

The superior performance of FedCVR over stateless baselines (FedAvg) and even standard adaptive configurations (FedYogi) is not merely a result of hyperparameter tuning, but rather a structural consequence of the interaction between server-side momentum and the Differential Privacy mechanism.

In a DP-FL system, every client update  $\Delta w_k$  contains two components: the true gradient signal  $\nabla L$  and the injected Gaussian noise  $\mathcal{N}(0, \sigma^2)$ . Stateless aggregators, such as FedAvg,

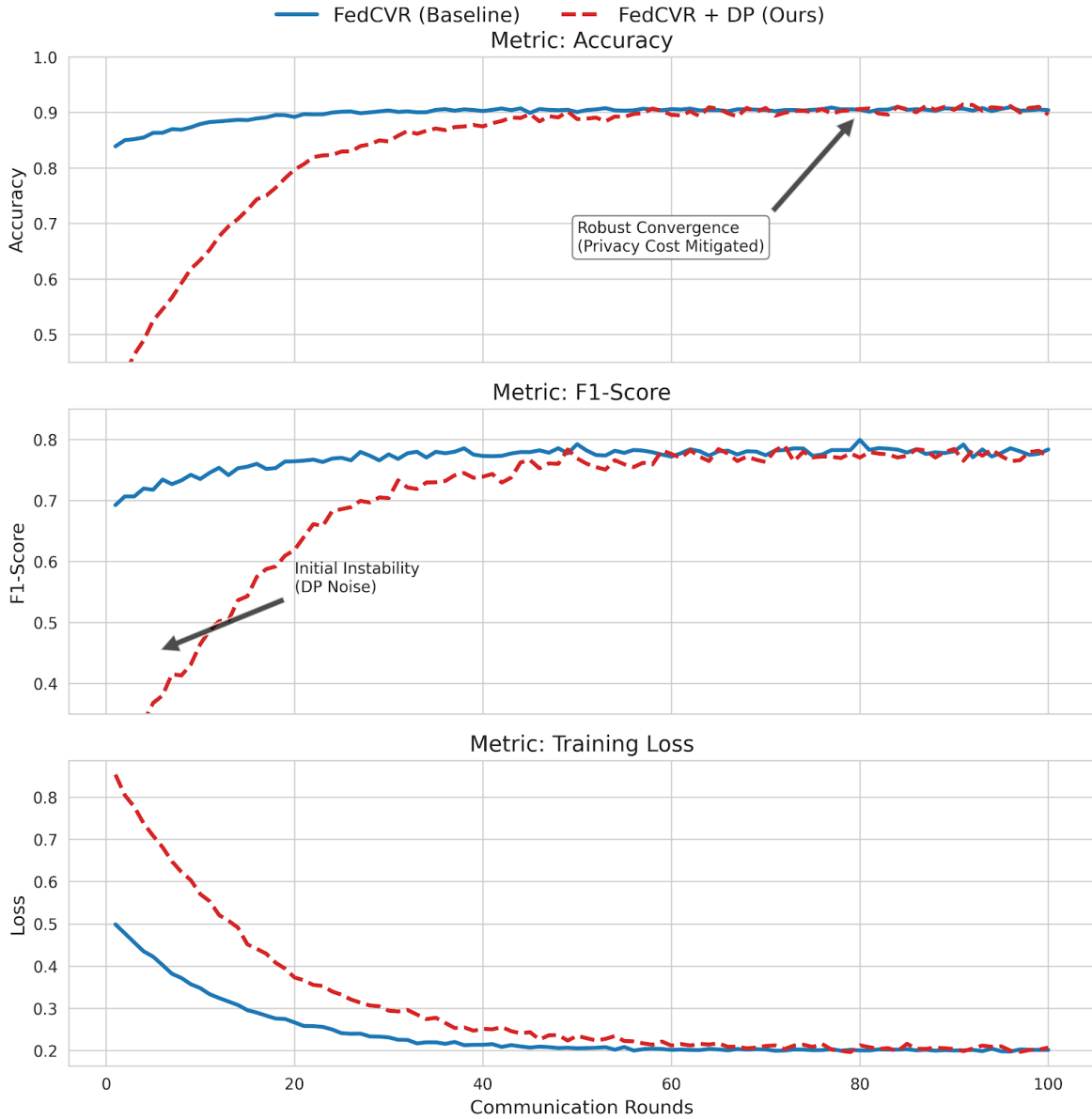


Figure 8: Impact of Differential Privacy on FedCVR Model Performance. The comparative analysis reveals two distinct phases: (1) an initial instability period (Rounds 0-30) caused by DP noise injection, followed by (2) a robust convergence phase where the FedCVR adaptive optimizer effectively filters the noise.

compute the arithmetic mean of these updates at each round  $t$ . Consequently, the global model  $w_{t+1}$  directly inherits the variance of the noise injected at round  $t$ , leading to the erratic convergence observed in our baselines.

In contrast, the adaptive aggregation logic employed in FedCVR introduces a **temporal filtering effect**. By maintaining a history of updates via the first moment vector  $m_t$ :

$$m_t = \beta_1 m_{t-1} + (1 - \beta_1)(g_{\text{signal}} + g_{\text{noise}}) \quad (21)$$

The system effectively averages out the zero-mean Gaussian noise over multiple rounds ( $\mathbb{E}[g_{\text{noise}}] \rightarrow 0$ ), acting as a **temporal denoiser**. Therefore, it allows the persistent clinical signal to accumulate while damping stochastic noise.

This mechanism also explains the performance advantage

over other adaptive methods. While FedCluster attempts to mitigate heterogeneity by grouping clients, it cannot filter against temporal gradient noise. Furthermore, compared to FedYogi, which employs a more aggressive additive update rule for the second moment, FedCVR's conservative moment estimation proved more robust to the "gradient explosion" often caused by the clipping operations inherent to DP-SGD.

## 9.2. Revisiting the Privacy-Utility Trade-off

A significant finding of this research is the re-evaluation of the "cost of privacy." Common literature suggests that implementing strong privacy guarantees ( $\epsilon < 10$ ) incurs a prohibitive performance cost. Our results challenge this assumption. While the analysis revealed predictable instability in the initial train-

ing rounds, the FedCVR aggregator demonstrated a remarkable capacity to recover utility.

Ultimately, the model converged to a performance plateau nearly identical to the non-private baseline in moderate privacy settings ( $\sigma = 1.0$ ). Even under high-privacy regimes, the degradation was graceful rather than catastrophic. Hence, implies that the trade-off is not a fixed barrier, but rather an engineering problem that can be solved through sophisticated optimization. By employing an aggregator that inherently dampens noise, we demonstrate that achieving formal privacy guarantees does not necessitate abandoning clinical utility.

### 9.3. Computational and Communication Overhead

From an engineering deployment perspective, the overhead introduced by FedCVR is minimal. While the server performs additional operations to calculate moments  $m_t$  and  $v_t$ , this computational cost is negligible compared to the network latency of transmitting model updates over the internet.

Crucially, the communication cost remains identical to FedAvg, as the vector sizes transmitted between the client and the server remain unchanged; the moment vectors are stored and updated solely on the server. The memory requirement on the server increases linearly by a factor of 3 (storing  $w_t, m_t, v_t$ ), which is trivial for modern server infrastructure, given the relatively small parameter space of tabular data models used in clinical risk scores.

### 9.4. Limitations

While this study demonstrates the engineering feasibility of the FedCVR framework, we acknowledge specific limitations inherent to its current validation scope:

- **Data Synthetic Nature:** We utilized synthesized data to precisely control the degree of statistical heterogeneity (Non-IID) and isolate the optimizer’s behavior. While this allows for rigorous ablation studies, it does not fully capture the missing values and unstructured noise that are typical of raw Electronic Health Records (EHRs).
- **Threat Model Scope:** Our privacy evaluation assumes an *honest-but-curious* threat model, focusing on mitigating inference attacks via Differential Privacy. The current framework does not implement Secure Multi-Party Computation (SMPC) or Secure Aggregation (SecAgg) to cryptographically hide individual updates from the server, nor does it address active Byzantine attacks (model poisoning).
- **Interoperability Assumptions:** The experiments assume a unified feature schema across all clients. In a real-world deployment involving heterogeneous hospital systems, a semantic interoperability layer (e.g., mapping local schemas to the HL7 FHIR standard) would be a necessary precursor to the federated training process.

## 10. Conclusion and Future Directions

In this work, we addressed the critical challenge of deploying robust Machine Learning models for cardiovascular risk prediction within a privacy-constrained, multi-institutional environment. We introduced and validated *FedCVR*, a framework designed to mitigate the adverse effects of Non-IID data distributions and Differential Privacy noise through server-side adaptive optimization. The following sections summarize our primary findings and outline strategic avenues for future research.

### 10.1. Conclusion

This study systematically evaluated the FedCVR framework against a comprehensive suite of baselines, including stateless aggregators (FedAvg and FedProx) and state-of-the-art adaptive optimizers (FedYogi and FedAdagrad). Our extensive empirical analysis on heterogeneous clinical data demonstrates that FedCVR significantly outperforms standard methods, achieving a final AUC of 0.96 and maintaining high clinical utility (Recall  $\approx 0.78$ ) even under moderate privacy budgets ( $\epsilon \approx 13.4$ ).

The results confirm that the specific momentum tuning in FedCVR acts as an effective *temporal denoiser*, filtering out the Gaussian noise injected by the privacy mechanism while preserving the true gradient signal. We conclude that for medical applications where data is statistically heterogeneous, and privacy is non-negotiable, simple aggregation is insufficient. Server-side adaptivity is a prerequisite for stabilizing training and ensuring the robust convergence of privacy-preserving AI models.

### 10.2. Future Directions

Building upon these findings, future research will expand the scope of this framework in four key directions:

- **Validation on Real-World Multi-Modal Data:** While this study validated the framework on structured clinical features, future work will transition to large-scale, real-world datasets (e.g., MIMIC-IV or eICU). Furthermore, we aim to incorporate multimodal data, combining tabular EHR data with unstructured clinical notes (NLP) or time-series signals (such as ECG) to enhance predictive accuracy.
- **Enhanced Security Layers:** The current privacy model focuses on Differential Privacy to prevent inference attacks. Future iterations will integrate cryptographic techniques, such as Secure Multi-Party Computation (SMPC) or Homomorphic Encryption, to protect the model updates themselves during transmission. Additionally, we will explore defense mechanisms against Byzantine failures and model poisoning attacks.
- **Personalized Federated Learning:** While FedCVR optimizes a single global model, clinical heterogeneity often requires localization. We plan to investigate Personalized Federated Learning (pFL) techniques, such as fine-tuning

the global model on local client data or learning client-specific headers, to further improve performance for specific patient demographics.

### Software and Data Availability

Data and source code will be made available on request.

### Conflict of Interest Statement

The authors declare that they have no known competing financial interests or personal relationships that could have influenced the work reported in this paper.

### Funding

This research did not receive any specific grant from funding agencies in the public, commercial, or not-for-profit sectors.

### References

- [1] A. Gaber, H. Abdeltwab, T. Elbatt, Fedcvd: Towards a scalable, privacy-preserving federated learning model for cardiovascular diseases prediction, in: Proceedings of the 2024 8th International Conference on Machine Learning and Soft Computing, ICMLSC '24, Association for Computing Machinery, New York, NY, USA, 2024, p. 7–11. doi:10.1145/3647750.3647752.
- [2] L. J. Laslett, P. Alagona, B. A. Clark, J. P. Drozda, F. Saldivar, S. R. Wilson, C. Poe, M. Hart, The worldwide environment of cardiovascular disease: prevalence, diagnosis, therapy, and policy issues: a report from the american college of cardiology, Journal of the American College of Cardiology 60 (25S) (2012) S1–S49.
- [3] E. O. Lopez, B. D. Ballard, A. Jan, Cardiovascular disease, in: StatPearls [Internet], StatPearls Publishing, 2023.
- [4] Abhishek, H. V. Bhagat, M. Singh, A machine learning model for the early prediction of cardiovascular disease in patients, in: 2023 Second International Conference on Advances in Computational Intelligence and Communication (ICACIC), 2023, pp. 1–5. doi:10.1109/ICACIC59454.2023.10435210.
- [5] A. Gupta, S. Misra, N. Pathak, D. Das, Fedcare: Federated learning for resource-constrained healthcare devices in iomt system, IEEE Transactions on Computational Social Systems 10 (4) (2023) 1587–1596.
- [6] A. Khimani, A. Hornback, N. Jain, P. Avula, A. Jaisankar, M. D. Wang, Predicting cardiovascular disease risk in tobacco users using machine learning algorithms, in: 2024 46th Annual International Conference of the IEEE Engineering in Medicine and Biology Society (EMBC), 2024, pp. 1–5. doi:10.1109/EMBC53108.2024.10782885.
- [7] S. Mittal, S. Gupta, K. Bansal, G. Aggarwal, Democratizing gdpr compliance: Ai-driven privacy policy interpretation, in: Proceedings of the 2024 Sixteenth International Conference on Contemporary Computing, IC3-2024, Association for Computing Machinery, New York, NY, USA, 2024, p. 735–743. doi:10.1145/3675888.3676142.
- [8] B. K. Jensen, M. Cline, C. S. Guynes, Hippa, privacy and organizational change: a challenge for management, SIG-CAS Comput. Soc. 37 (1) (2007) 12–17. doi:10.1145/1273353.1273354.
- [9] S. M. Shah, R. A. Khan, Secondary use of electronic health record: Opportunities and challenges, IEEE Access 8 (2020) 136947–136965. doi:10.1109/ACCESS.2020.3011099.
- [10] H. B. McMahan, E. Moore, D. Ramage, B. A. y Arcas, Federated learning of deep networks using model averaging, CoRR abs/1602.05629 (2016). arXiv:1602.05629. URL <http://arxiv.org/abs/1602.05629>
- [11] H. Wang, Z. Kaplan, D. Niu, B. Li, Optimizing federated learning on non-iid data with reinforcement learning, in: IEEE INFOCOM 2020 - IEEE Conference on Computer Communications, 2020, pp. 1698–1707. doi:10.1109/INFOCOM41043.2020.9155494.
- [12] K. Thumula, H. Holla, C. Gutti, A. A. Sasikumar, H. Gogineni, Privfed: Protecting user privacy in federated learning systems through differential privacy, in: 2025 8th International Conference on Electronics, Materials Engineering & Nano-Technology (IEMENTech), 2025, pp. 1–6. doi:10.1109/IEMENTech65115.2025.10959665.
- [13] S. Ahmed, M. S. Kaiser, S. Chaki, S. Aloteibi, M. A. Moni, Federated learning model with dynamic scoring-based client selection for diabetes diagnosis, Knowledge-Based Systems 320 (2025) 113662. doi:https://doi.org/10.1016/j.knosys.2025.113662.
- [14] A. Silverio, P. Cavallo, R. De Rosa, G. Galasso, Big health data and cardiovascular diseases: A challenge for research, an opportunity for clinical care, Frontiers in Medicine Volume 6 - 2019 (2019). doi:10.3389/fmed.2019.00036. URL <https://www.frontiersin.org/journals/medicine/articles/10.3389/fmed.2019.00036>
- [15] Z. Qu, X. Zhao, L. Sun, G. Muhammad, Daqfl: Dynamic aggregation quantum federated learning algorithm for intelligent diagnosis in internet of medical things, IEEE Internet of Things Journal (2025) 1–1doi:10.1109/JIOT.2025.3537614.
- [16] L. Qiu, J. Cheng, H. Gao, W. Xiong, H. Ren, Federated semi-supervised learning for medical image segmentation via pseudo-label denoising, IEEE journal of biomedical and health informatics 27 (10) (2023) 4672–4683.

- [17] F. Ullah, G. Srivastava, H. Xiao, S. Ullah, J. C.-W. Lin, Y. Zhao, A scalable federated learning approach for collaborative smart healthcare systems with intermittent clients using medical imaging, *IEEE Journal of Biomedical and Health Informatics* (2023).
- [18] K. Benitez, B. Malin, Evaluating re-identification risks with respect to the hipaa privacy rule, *Journal of the American Medical Informatics Association* 17 (2) (2010) 169–177.
- [19] S. Goto, D. Solanki, J. E. John, R. Yagi, M. Homilius, G. Ichihara, Y. Katsumata, H. K. Gaggin, Y. Itabashi, C. A. MacRae, R. C. Deo, Multinational federated learning approach to train ecg and echocardiogram models for hypertrophic cardiomyopathy detection, *Circulation* 146 (10) (2022) 755–769. doi:10.1161/CIRCULATIONAHA.121.058696.
- [20] N. T. Madathil, F. K. Dankar, M. Gergely, A. N. Belkacem, S. Alrabaae, Revolutionizing healthcare data analytics with federated learning: A comprehensive survey of applications, systems, and future directions, *Comput. Struct. Biotechnol. J.* 28 (2025) 217–238.
- [21] M. J. Sheller, B. Edwards, G. A. Reina, J. Martin, S. Pati, A. Kotrotsou, M. Milchenko, W. Xu, D. Marcus, R. R. Colen, et al., Federated learning in medicine: facilitating multi-institutional collaborations without sharing patient data, *Scientific reports* 10 (1) (2020) 12598.
- [22] S. Pati, U. Baid, B. Edwards, M. Sheller, S.-H. Wang, G. A. Reina, P. Foley, A. Gruzdev, D. Karkada, C. Davatzikos, et al., Federated learning enables big data for rare cancer boundary detection, *Nature communications* 13 (1) (2022) 7346.
- [23] A. Linardos, K. Kushibar, S. Walsh, P. Gkontra, K. Lekadir, Federated learning for multi-center imaging diagnostics: a simulation study in cardiovascular disease, *Scientific Reports* 12 (1) (2022) 3551.
- [24] K. Bharathi, Dhavamani, Niranjana, A federated learning based approach for heart disease prediction, in: 2022 6th International Conference on Computing Methodologies and Communication (ICCMC), 2022, pp. 1117–1121. doi:10.1109/ICCMC53470.2022.9754119.
- [25] J. Wang, J. Gounley, H. Hanson, Cafe au lait: Compute-aware federated augmented low-rank ai training, in: Proceedings of the Platform for Advanced Scientific Computing Conference, PASC '25, Association for Computing Machinery, New York, NY, USA, 2025, p. 1–12. doi:10.1145/3732775.3733580.
- [26] P. J. Maliakel, S. Ilager, I. Brandic, Fligan: Enhancing federated learning with incomplete data using gan, in: Proceedings of the 7th International Workshop on Edge Systems, Analytics and Networking, EdgeSys '24, Association for Computing Machinery, New York, NY, USA, 2024, p. 1–6. doi:10.1145/3642968.3654813.
- [27] A. Dhasade, Y. Ding, S. Guo, A.-M. Kermarrec, M. de Vos, L. Wu, Quickdrop: Efficient federated unlearning via synthetic data generation, in: Proceedings of the 25th International Middleware Conference, Middleware '24, Association for Computing Machinery, New York, NY, USA, 2024, p. 266–278. doi:10.1145/3652892.3700764.
- [28] S. Maddock, G. Cormode, C. Maple, Flaim: Aim-based synthetic data generation in the federated setting, in: Proceedings of the 30th ACM SIGKDD Conference on Knowledge Discovery and Data Mining, KDD '24, Association for Computing Machinery, New York, NY, USA, 2024, p. 2165–2176. doi:10.1145/3637528.3671990.
- [29] A. R. Ghavamipour, F. Turkmen, R. Wang, K. Liang, Federated synthetic data generation with stronger security guarantees, in: Proceedings of the 28th ACM Symposium on Access Control Models and Technologies, SACMAT '23, Association for Computing Machinery, New York, NY, USA, 2023, p. 31–42. doi:10.1145/3589608.3593835.
- [30] N. Rieke, J. Hancox, W. Li, F. Milletari, H. R. Roth, S. Albarqouni, S. Bakas, M. N. Galtier, B. A. Landman, K. Maier-Hein, et al., The future of digital health with federated learning, *NPJ digital medicine* 3 (1) (2020) 119.
- [31] S. Banerjee, S. Barik, D. Das, U. Ghosh, Ehr security and privacy aspects: A systematic review, in: IFIP International Internet of Things Conference, Springer, 2023, pp. 243–260.
- [32] A. Hudaib, N. Obeid, A. Albashayreh, H. Mosleh, Y. Tashtoush, G. Hristov, Exploring the implementation of federated learning in healthcare: a comprehensive review, *Cluster Comput.* 28 (5) (Oct. 2025).
- [33] S. Ahmed, M. S. Kaiser, S. Chaki, S. Aloteibi, M. A. Moni, Federated learning model with dynamic scoring-based client selection for diabetes diagnosis, *Knowl. Based Syst.* 320 (113662) (2025) 113662.
- [34] B. Yurdem, M. Kuzlu, M. K. Gullu, F. O. Catak, M. Tabasum, Federated learning: Overview, strategies, applications, tools and future directions, *Heliyon* 10 (19) (2024) e38137. doi:https://doi.org/10.1016/j.heliyon.2024.e38137.
- [35] T. An, L. Ma, W. Wang, Y. Yang, J. Wang, Y. Chen, Consideration of fedprox in privacy protection, *Electronics* 12 (20) (2023). doi:10.3390/electronics12204364. URL https://www.mdpi.com/2079-9292/12/20/4364
- [36] C. You, Z. Lu, J. Wang, C. Yan, Fedddb: Clustered federated learning based on data distribution difference, in: Proceedings of the 2022 5th International Conference on Algorithms, Computing and Artificial Intelligence, ACAI '22, Association for Computing Machinery, New York,

- NY, USA, 2023. doi:10.1145/3579654.3579732. URL <https://doi.org/10.1145/3579654.3579732>
- [37] S. Reddi, Z. Charles, M. Zaheer, Z. Garrett, K. Rush, J. Konečný, S. Kumar, H. B. McMahan, *Adaptive federated optimization* (2021). arXiv:2003.00295. URL <https://arxiv.org/abs/2003.00295>
- [38] Y. Luo, Z. Pan, Q. Fu, S. Qin, Fadagrad: Adaptive federated learning with differential privacy, in: 2024 IEEE International Conference on High Performance Computing and Communications (HPCC), 2024, pp. 508–515. doi:10.1109/HPCC64274.2024.00074.
- [39] X. Xing, H. Liu, Adaptive federated learning with high-efficiency communication compression, in: 2024 43rd Chinese Control Conference (CCC), 2024, pp. 1903–1909. doi:10.23919/CCC63176.2024.10661207.
- [40] P. M. Mammen, *Federated learning: Opportunities and challenges*, CoRR abs/2101.05428 (2021). arXiv:2101.05428. URL <https://arxiv.org/abs/2101.05428>
- [41] C. Beguier, J. O. du Terrail, I. Meah, M. Andreux, E. W. Tramel, *Differentially private federated learning for cancer prediction* (2021). arXiv:2101.02997. URL <https://arxiv.org/abs/2101.02997>
- [42] Y. Li, T.-H. Chang, C.-Y. Chi, Secure federated averaging algorithm with differential privacy, in: 2020 IEEE 30th International Workshop on Machine Learning for Signal Processing (MLSP), 2020, pp. 1–6. doi:10.1109/MLSP49062.2020.9231531.
- [43] J. Tang, Fedacc algorithm based on client accuracy in federated learning, in: 2024 5th International Conference on Computer Engineering and Intelligent Control (ICCEIC), 2024, pp. 256–260. doi:10.1109/ICCEIC64099.2024.10775793.
- [44] Y. Fu, T. Wang, Benchmarking secure sampling protocols for differential privacy, in: Proceedings of the 2024 on ACM SIGSAC Conference on Computer and Communications Security, CCS '24, Association for Computing Machinery, New York, NY, USA, 2024, p. 318–332. doi:10.1145/3658644.3690257.
- [45] Q. Liu, R. Shakya, M. Khalil, J. Jovanovic, Advancing privacy in learning analytics using differential privacy, in: Proceedings of the 15th International Learning Analytics and Knowledge Conference, LAK '25, Association for Computing Machinery, New York, NY, USA, 2025, p. 181–191. doi:10.1145/3706468.3706493.
- [46] J. Birrell, R. Ebrahimi, R. Behnia, J. Pacheco, Differentially private stochastic gradient descent with fixed-size minibatches: tighter rdp guarantees with or without replacement, in: Proceedings of the 38th International Conference on Neural Information Processing Systems, NIPS '24, Curran Associates Inc., Red Hook, NY, USA, 2025.
- [47] Y. Zhang, Q. Ye, H. Hu, Federated heavy hitter analytics with local differential privacy, Proc. ACM Manag. Data 3 (1) (Feb. 2025). doi:10.1145/3709739.
- [48] A. Di Fazio, Enhancing privacy in recommender systems through differential privacy techniques, in: Proceedings of the 18th ACM Conference on Recommender Systems, RecSys '24, Association for Computing Machinery, New York, NY, USA, 2024, p. 1348–1352. doi:10.1145/3640457.3688019.
- [49] A. Koskela, J. Jälkö, A. Honkela, Computing tight differential privacy guarantees using fft, in: International Conference on Artificial Intelligence and Statistics, PMLR, 2020, pp. 2560–2569.
- [50] A. Yousefpour, I. Shilov, A. Sablayrolles, D. Testuggine, K. Prasad, M. Malek, J. Nguyen, S. Ghosh, A. Bharadwaj, J. Zhao, et al., Opacus: User-friendly differential privacy training in pytorch, arXiv preprint arXiv:2109.12298 (2022). doi:https://doi.org/10.48550/arXiv.2109.12298.
- [51] C. Dwork, A. Roth, The algorithmic foundations of differential privacy, Foundations and Trends® in Theoretical Computer Science 9 (3–4) (2014) 211–407.
- [52] A. Maurya, R. Haripriya, M. Pandey, J. Choudhary, D. Pratap Singh, S. Solanki, D. Sharma, Federated Learning for Privacy-Preserving Severity Classification in Healthcare: A Secure Edge-Aggregated Approach, IEEE Access 13 (2025) 102339–102358. doi:10.1109/ACCESS.2025.3576135.
- [53] Z. Ruan, X. Dong, J. Shen, Z. Cao, Mc-dqe fl: Robust federated learning framework based on multi-criteria data quality evaluation, in: 2025 IEEE 6th International Seminar on Artificial Intelligence, Networking and Information Technology (AINIT), 2025, pp. 913–917. doi:10.1109/AINIT65432.2025.11035735.
- [54] K. Shivaprasad, A. Wadhawan, Deep learning-based plant leaf disease detection, in: 2023 7th International Conference on Intelligent Computing and Control Systems (ICICCS), 2023, pp. 360–365. doi:10.1109/ICICCS56967.2023.10142857.
- [55] A. Ali, A. Arafa, Delay sensitive hierarchical federated learning with stochastic local updates, IEEE Transactions on Cognitive Communications and Networking (2025) 1–1doi:10.1109/TCCN.2025.3527699.
- [56] S. Savazzi, M. Nicoli, V. Rampa, S. Kianoush, Federated learning with mutually cooperating devices: A consensus approach towards server-less model optimization, in: ICASSP 2020 - 2020 IEEE International Conference on Acoustics, Speech and Signal Processing (ICASSP), 2020, pp. 3937–3941. doi:10.1109/ICASSP40776.2020.9054055.

- [57] N. Nezhadsistani, N. S. Moayedian, B. Stiller, Blockchain-enabled federated learning in healthcare: Survey and state-of-the-art, *IEEE Access* (2025).
- [58] M. Chen, Y. Hao, K. Hwang, L. Wang, L. Wang, Disease prediction by machine learning over big data from healthcare communities, *IEEE access* 5 (2017) 8869–8879.
- [59] Y. Ruan, X. Zhang, C. Joe-Wong, How valuable is your data? optimizing client recruitment in federated learning, *IEEE/ACM Trans. Netw.* 32 (5) (2024) 4207–4221. doi:10.1109/TNET.2024.3422264.
- [60] A. Bhardwaj, Framingham heart study dataset, <https://www.kaggle.com/datasets/aasheesh200/framingham-heart-study-dataset>, accessed: Apr. 24, 2023 (Apr. 2022).
- [61] M. Siddhartha, Heart disease dataset (comprehensive) (2020). doi:10.21227/dz4t-cm36.
- [62] R. Detrano, Cleveland heart disease dataset, <https://archive.ics.uci.edu/ml/datasets/Heart+Disease>, uCI Machine Learning Repository. Accessed: Jul. 26, 2024 (1988).
- [63] A. Janosi, Hungarian heart disease dataset, <https://archive.ics.uci.edu/ml/datasets/Heart+Disease>, uCI Machine Learning Repository. Accessed: Jul. 26, 2024 (1988).
- [64] A. A. Khan, The heart failure prediction dataset: Fic pakistan, <https://www.kaggle.com/datasets/asgharalikhan/mortality-rate-heart-patient-pakistan-hospital>, accessed: Sep. 18, 2024 (2022).
- [65] M. Dubey, J. Tembhurne, R. Makhijani, Enhancing federated learning through differential privacy: Introducing FedHybrid for multicenter diverse heart disease datasets, *IEEE Trans. Emerg. Top. Comput. Intell.* (2025) 1–14.
- [66] W. Zhang, Diabetes detection: Predicting type ii diabetes with machine learning algorithm, in: *Proceedings of the 2025 International Conference on Health Big Data, HBD '25*, Association for Computing Machinery, New York, NY, USA, 2025, p. 16–22. doi:10.1145/3733006.3733009.
- [67] A. E. W. Johnson, T. J. Pollard, L. Shen, L.-W. H. Lehman, M. Feng, M. Ghassemi, B. Moody, P. Szolovits, L. A. Celi, R. G. Mark, MIMIC-III, a freely accessible critical care database, *Sci. Data* 3 (1) (2016) 160035.
- [68] F. K. Dankar, N. Madathil, Using synthetic data to reduce model convergence time in federated learning, in: *Proceedings of the 2022 IEEE/ACM International Conference on Advances in Social Networks Analysis and Mining, ASONAM '22*, IEEE Press, 2023, p. 293–297. doi:10.1109/ASONAM55673.2022.10068615.
- [69] M. Naseri, J. Fernandez-Marques, Y. Gao, H. Pan, Privacy-preserving federated learning using flower framework, in: *Proceedings of the 30th ACM SIGKDD Conference on Knowledge Discovery and Data Mining, KDD '24*, Association for Computing Machinery, New York, NY, USA, 2024, p. 6422–6423. doi:10.1145/3637528.3671447.
- [70] E. Stevens, L. P. G. Antiga, T. Viehmann, Vol. Electronic ISBN:9781617295263, 2020. [link]. URL <http://ieeexplore.ieee.org/document/10280272>
- [71] F. Pedregosa, G. Varoquaux, A. Gramfort, V. Michel, B. Thirion, O. Grisel, M. Blondel, P. Prettenhofer, R. Weiss, V. Dubourg, J. Vanderplas, A. Passos, D. Cournapeau, M. Brucher, M. Perrot, E. Duchesnay, Scikit-learn: Machine learning in python, *J. Mach. Learn. Res.* 12 (null) (2011) 2825–2830.
- [72] C. R. Harris, K. J. Millman, S. J. van der Walt, R. Gommers, P. Virtanen, D. Cournapeau, E. Wieser, J. Taylor, S. Berg, N. J. Smith, R. Kern, M. Picus, S. Hoyer, M. H. van Kerkwijk, M. Brett, A. Haldane, J. F. Del Río, M. Wiebe, P. Peterson, P. Gérard-Marchant, K. Sheppard, T. Reddy, W. Weckesser, H. Abbasi, C. Gohlke, T. E. Oliphant, Array programming with NumPy, *Nature* 585 (7825) (2020) 357–362. doi:https://doi.org/10.1038/s41586-020-2649-2.